6-1-2017

Characterization of aggresome formation in choroid plexus carcinoma.

Marwa Mohamed Ali Nassar

The American University in Cairo
School of Science and Engineering
Applied Sciences Program

Characterization of Aggresome Formation in Choroid Plexus Carcinoma.

A Thesis Submitted to
The Applied Sciences Graduate Program.

In partial fulfilment of the requirements for
the degree of Doctorate of Philosophy

by Marwa Mohamed Ali Nassar
Msc of Microbiology and Immunology- Faculty of Pharmacy, Cairo University
Bachelor of Pharmacy- Cairo University

Under the supervision of Dr.Shahenda El-Naggar

Head of Basic Research, Children Cancer Hospital 57357

And Dr. Ahmed Moustafa

Associate Professor of Bioinformatics, American University in Cairo

March 2017

TABLE OF CONTENTS

ACKNOWLEDGEMENT

I sincerely thank Dr.Shahenda El-Naggar my main supervisor for her support and effort throughout my thesis. Dr.Ahmed Moustafa my academic advisor for his advising and guidance. I would also like to acknowledge the following people for all the assistance and support they have given me: Myret Ghabriel for introducing me to the cell culture and her innovative technique with bisulfite sequencing. Heba Samaha for troubleshooting and finishing the transfection experiment. Finally, I would like to thank the pathology team under supervision of Dr Hala Taha, at the Children Cancer Hospital Egypt 57357 for all the immunohistochemistry assays.

I am really grateful to The Youssef Gameel Fellowship for supporting the first years of my PhD. This work was supported by TWAS (The World Academy of Science), L'Oreal Women in Science Fellowship Award and STDF (The Science and Technology Development Fund).

Lastly, I would like to thank my parents for their love and encouragement. My husband for his great support, Hussein and Layla, this work is dedicated to you.

List of Abbreviations

Abbreviation	Meaning
ACPP	Atypical Choroid plexus papilloma
AD	Alzheimer's disease
ALS	Amyotrophic lateral sclerosis
AMPK	AMP dependent kinase
ARF	ADP-ribosylation factor
ATG	Autophagy related protein
ATM	ATM serine therionine kinase
ATP	Adenosine triphosphate
5-AZa-dC	5-Aza-2′-deoxycytidine
BRCA-1	Breast Cancer type 1
CBRTUS	Central Brain Tumor Registry of the United States
ChK2	Checkpoint kinase 2
CNS	Central nervous system
CMA	Chaperone mediated autophagy
CMV	Cytomegalovirus
CPC	Choroid plexus carcinoma
CPP	Choroid plexus papilloma
CPT	Choroid plexus tumors
CNS	Central nervous system
CSF	Cebrospinal fluid
CT	Computed tomography
DBM	Dynenin binding domain
DNA	Deoxyribonucleic acid
E1	Ubiquitin activating enzyme
E2	Ubiquitin conjugating enzyme
E3	Ubiquitin ligase
ESCC	Oesophageal squamous cell carcinoma
FDA	Food and drug administration
FFPE	Formalin fixed and paraffin embedded
FKBP-12	FK506 binding protein
GABARAP	γ-AminoButyrate acid receptor-associated protein
GABARAP	GABARAP-like protein
GBM	Glioblastoma multiform
GFP	Green fluorescence protein
HAT	Histone acetyl transferase
HD	Huntington's disease
HDACs	Histone deacetylases
HDAC6	Histone deactylase 6
IF	Intermediate filament
INQ	Intra nuclear quality control
IPOD	Insoluble protein deposit
JUNQ	Juxtanuclear quality control
LAMP	Lysosomal-associated membrane protein
LC3	Microtubule-associated protein light chain 3

LFS	Li Fraumeni syndrome
MCA	Multiplex cell authentication
MGMT	Methyl guanine-DNA methyl transferase
MiRNA	Micro RNA
mLST8	Target of rapamycin complex subunit LST8
MRI	Magnetic resonance imaging
MTOC	Microtubule organizing centre
mTOR	Mammalian target of rapamycin
P62/SQSTM1	ubiquitin-binding protein p62/ Sequestosome-1
PAS	Phagophore assembly site
PDGFR	Platelet derived factor receptor
PE	Phosphatidylethanolamine
PI3K	Phosphatidylinositol 3-kinases
PNET	Primitive neuroectodermal tumors
PRAS-40	Proline-rich Akt substrate of 40 kDa
PPR5	Proline rich 5
PROTOR-1	Protein observed with Rictor-1
RNA	Ribonucleic acid
RICTOR	Rapamycin-insensitive companion of mammalian target of rapamycin
S6K	Shaggy-related protein kinase 6
SHSY-5Y	Neuroblastoma cell line
SOD	Superoxide dismutase
TP53	Tumor protein 53
Ub	Ubiquitin
UPS	Ubiquitin proteasome system
UVRAG	UV radiation resistance-associated gene protein
WHO	World health organization

List of Figures:

List of Tables:

ABSTRACT

Protein misfolding is inevitable, 30% of newly synthesized polypeptides can end up misfolded, and such proteins are either refolded or eliminated by cellular quality control pathways. These pathways include the ubiquitin proteosome system and autophagy. In recent years, protein misfolding has been implicated in the pathophysiology of many diseases such as diabetes, neurological disorders and cancer. Studies from our laboratory have shown that choroid plexus carcinoma tumors are characterized by the formation of aggresomes at the microtubules organizing centers (MTOC) in formalin fixed and paraffin embedded (FFPE) tumor tissues. This was further confirmed by the development of choroid plexus carcinoma cell line (CCHE-45) which was characterized by the constitutive formation of aggresomes at MTOC. Aggresome formation implies presence of toxic protein over load and/or defective autophagy. The role of autophagic flux in the removal of aggresomes was further investigated. CCHE-45 cells displayed an increase in both basal and induced autophagic flux. Furthermore, microtubule-associated protein light chain 3 A- variant 1 (LC3A-V1) expression was silenced by promoter methylation in these cells. Restoring LC3A-V1 resulted in the elimination of the aggresomes and the recruitment of Lysosomal-Associated Membrane Protein (LAMP2) independent from autophagosome formation. Based on these findings we suggest that quality control autophagy in CCHE-45 is mediated by LC3A in aggresomes clearance. We propose that perturbation in the autophagic pathway by the absence of LC3A expression leads to a failure in aggresome degradation thus overcoming misfolded protein overload.

AIM OF THE STUDY

Thirty percent of newly synthesized polypeptides can end up misfolded, such proteins are either refolded or eliminated by cellular quality control pathways which include the ubiquitin proteosome system and autophagy. When misfolded proteins exceed the ability of cell quality control to be eliminated they may end up in storage compartments. Aggresomes are juxtanuclear protein aggregates which act as a storage bins for misfolded proteins. In children Cancer hospital 57357 a new choroid plexus carcinoma cell line CCHE-45 was established. The cells were characterized by the presence of a single cage like inclusion body at juxtanuclear position that was positive for vimentin. These structures have been identified previously as aggresomes. The aim of the study is to characterize the mechanisms underlying aggresomes clearance in choroid plexus carcinoma.

1-LITERATURE REVIEW

1.1 Tumor Biology:

Cancer is a term that encompasses a wide class of diseases, but mainly it is used to describe disorders that are characterized by abnormal new growth or "neoplasm" formation. The ability of a neoplasm to invade the surrounding tissues or its invasive capacity is what governs the tendency of the tumor to be malignant and gives it the ability to further metastasize through blood or lymphatic vessel (Bunz, 2008). Genetic analysis on both chromosomal and DNA levels has revealed that neoplasms mainly originate from a single cell in what is known as the monoclonal origin of cancer cells (Nowell, Rowley, & Knudson, 1998). In the late seventies, it was hypothesized that the monoclonal cancer cell has a selective advantage which favours its selection and allow it to proliferate and overcome the neighbouring cells (Nowell, 1976). Later studies showed that cancer cells acquire genomic instability and accumulated changes in multiple genes which imply that more than a single event is required for tumorigenesis (Lengauer, Kinzler, & Vogelstein, 1998). These aberrations usually occur either spontaneously on a somatic level or hereditary through germ line mutations. Germ line cancers represent a small percentage (around 10%) of human cancers. Unlike somatic gene mutations, germ line cancer genes are vertically transferred in every cell of the carrier (Bunz, 2008).

The accumulation of genetic and /or epigenetic aberrations lead to an acquisition of a number of survival mechanisms, hence enabling the tumor to grow and metastasis and most importantly evade apoptosis (Virani, Colacino, Kim, & Rozek, 2013). In addition to blocking the growth suppression mechanisms mainly involving tumor suppressor genes, inducing angiogenesis, indefinite proliferation, immortality and acquiring a strong capability for invasion and bypassing the immune system in what is known as the hallmarks of cancer (Hanahan & Weinberg, 2011).

1.2 Genetic changes contributing to cancer:

On the genetic level, cancer may arise from genetic modification in either a proto-oncogene or a tumor suppressor gene. A proto -oncogene mutation leads to expression of a protein of a higher biochemical activity than its non-mutated counterpart, resulting in an alteration in cancer cell growth and differentiation (Camaco, 2012). Oncogenes encode proteins that play different roles such as transcription factors, growth factors, growth factors receptors, signal transduction or chromatin remodelling (Croce, 2008). The RAS gene family was among the first oncogenes discovered in cancer. The RAS family includes (H-ras, N-ras and K-ras) (Tabin & Weinberg, 1985). High mutation frequencies in these genes were reported in pancreatic, colorectal and lung carcinomas. Other common oncogenes includes MLL, BCL2, C-MYC and the ERRB families (Camaco, 2012).

On the other hand, tumor suppressor genes mutation is characterized by loss of function that leads to perturbations in the cell cycle, genetic instability and apoptosis and ultimately results in disruption of homeostasis inside the cell. Mutation in the *RB* gene in retinoblastoma, the *APC* gene in colorectal cancer and the *TP53* gene are common examples of tumor suppressor genes frequently mutated in cancer (Bunz, 2008).

The most intensively studied tumor suppressor gene is the TP53 which is highly mutated in several human malignancies. TP53 was first discovered in 1979 by Levine and Crawford (Lane & Crawford, 1979; Linzer, Maltzman, & Levine, 1979). Few years later the gene was located on the short arm of chromosome 17 (Muleris, Salmon, Zafrani, Girodet, & Dutrillaux, 1985). TP53 mutation could be either somatic or inherited. Germ line mutations in TP53 is inherited in families in what is known as Li Fraumeni syndrome (LFS) leading to predisposition to bone, brain especially choroid plexus carcinoma, lung and a number of soft tissue scarcomas (Kamihara, Rana, & Garber, 2014). Table 1 and 2 shows tumors associated with somatic and germ line mutations in TP53.

Cancer type	Prevalence
Colorectal	43.28%
Head and neck	42.51%
Esophagus	41.21%
Female genital cancer	38.57%
Pancreatic	34.67%
Skin	34.53%
Stomach	32.38%
Liver	31.16%
Urinary tract	28.87%
Nervous system	25.95%
Breast	22.81%
Soft tissues	21.38%
Lymph nodes	19.34%
Male genital	16.38%
Endocrine glands	15%
Bones	14.43%

Table (1): Tumors associated with somatic mutation of TP53 according to IARC TP53 mutation database, R17 release. TP53 mutation prevalence by tumor site, https://www.iarc.fr/

Cancer type	Prevalence
Breast	27.61%
Soft tissues	13.6%
Brain	12.03%
Adrenal gland	10.01%
Other	6.69%
Bones	6.69%
Hematological	3.77%
Colorectal	2.9%
Skin	2.65%

Table (2): Tumors associated with TP53 germ line mutations according to IARC TP53 mutation database, R17 release. TP53 mutation prevalence by tumor site. https://www.iarc.fr/

1.2.1:Tp53 function:

TP53 is a transcription factor with an estimated 3,600 genes under its regulation (Li, et al., 2012). Stressors such as DNA damage, hypoxia, pH change or starvation stimulate a number of TP53 upstream mediators such as ATM, ARF and ChK2. The mediators facilitate the up regulation of p53 through the dissociation of the P53 from its negative regulators; MDM2 an E3 ubiquitin ligase. The P53activation leads to either cell cycle arrest in G1 or G2 phase and or apoptosis (Kamihara, Rana, & Garber, 2013).

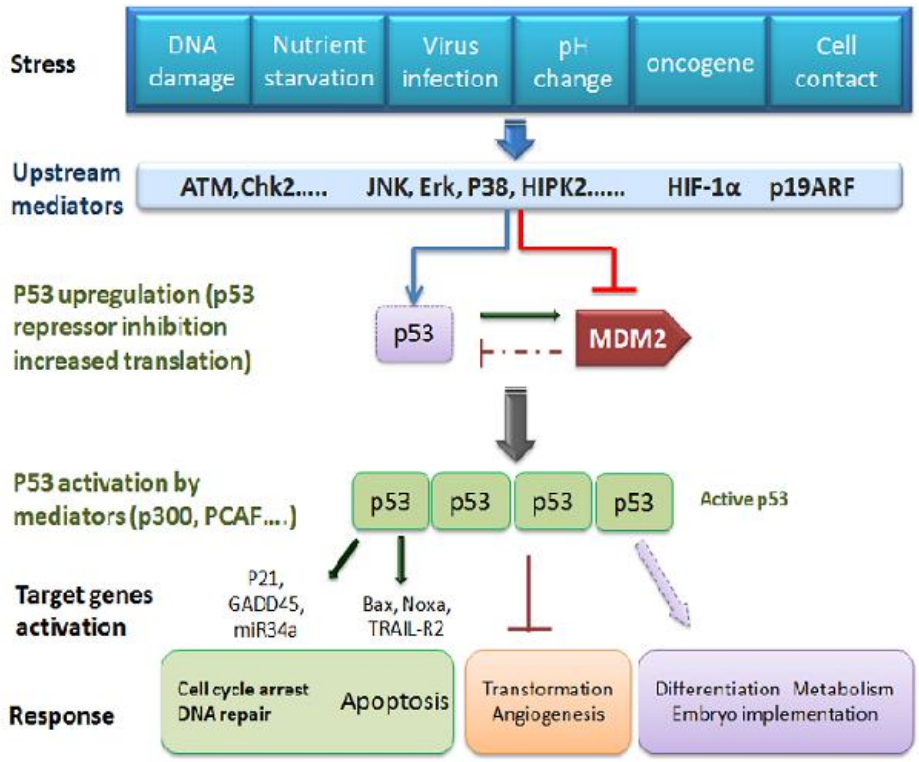

Figure (1): Schematic illustration of P53 pathway showing different stresses that stimulate TP53 upstream mediators such as ATM, ARF and ChK2. The mediators facilitate dissociation of P53 from its negative regulators, leading to different responses (Surget, Khoury & Bourdan, 2013).

1.3 Epigenetic changes contributing to cancer:

Epigenetic changes associated with cancer are changes in gene expression pattern independent on DNA sequence. These changes are generated by modification events in the DNA molecule such as post translational histone modification, DNA hypo or hypermethylation or changes in a micro RNA level (Sharma, Kelly, & Jones, 2010). With hopes of restoring normal functions of genes, epigenetic therapy is a new promising field in cancer treatment based on the reversibility of epigenetic mark. Currently several FDA approved drugs are used in cancer treatment including Temozolamide, Azacitidine and Decitabine (Ho, Turcan, & Chan, 2013; Sharma, et al., 2010).

The three main epigenetic events contributing to cancer will be discussed further.

1 .3.1 Non coding microRNA:

Micro RNAs (miRNA) are non-coding single stranded RNA molecules approximately 22 nucleotides long (Sharma, et al., 2010). miRNA has a role in regulating posttranscriptional gene expression. Around 1000 micro RNA have been reported so far which down regulate the translation of around 60% of protein coding mRNA (Friedman, Farh, Burge, & Bartel, 2009). In recent years, it is becoming evident that miRNA regulate many cellular process including development, cell proliferation and apoptosis. In addition to regulating several cellular processes, miRNA are have been linked several diseases including cancer (Kanwal & Gupta, 2012). A list of altered miRNA reported in human cancers include miR21 over expression in glioblastoma, prostate and lung cancer, miR-34b/34c up regulation in colon cancer, miR-125 up regulation in breast cancer, miR-221 and miR-222 down regulation in hepatocellular carcinoma and miR-92b up regulation in primary brain tumors (Kanwal & Gupta, 2012). Furthermore, miRNA expression profile is now used for cancer classification (Lu, et al., 2005).

1.3.2 Histone modifications:

In eukaryotes, the wrapping of the DNA around the histone proteins forming the nucleosome packs the large genome into the nucleus while still ensuring appropriate access to it for correct gene expression. The nucleosome core have an estimated 147 base pairs wrapped around a histone octamer formed of 2 copies of the highly conserved H2A, H2B, H3, H4 histones (Henikoff & Ahmad, 2005). Histones have flexible N-terminus known as the histone tail, which is susceptible to a number of covalent modifications such as acetylation, methylation, phosphorylation and ubiquitination. Such modifications either allow formation of the transcriptionally inactive compact heterochromatin or the open active euchromatin.
trimethylation of H3K4, H3K36 and H3K79 is characteristic of euchromatin, while methylation of H3K9, H3K27 and H4K20 is present in heterochromatin (Kanwal & Gupta, 2012). A histone code is another epigenetic modification that regulates many DNA processes including repair, regulation of gene expression, replication, centromere and telomere maintenance. Recent research brought to light a number of mutations in genes that affect histones post-translational modifications such as histone deacetylases, methyltransferases, acetyl transferases and demethylases (Chi, Allis, & Wang, 2010). Furthermore, changes in histone pattern of covalent modification such as increased H3K4 dimethylation or H3K18 acetylation have been linked to poor prognosis in cancer (Myzak & Dashwood, 2006).

1.3.3 CpG island and DNA methylation:

CpG islands are short distinctively interspersed DNA sequences around 1000 base pairs (bp) in length. They are characterized by having a rich CG base composition; this phenomenon enables DNA methyltransferase to covalently attach a methyl group to 5^{th} carbon atom of cytosine ring situated next to a guanine nucleotide forming the CpG islands (Bunz, 2008; Sharma, et al., 2010).

CpG islands are often present in transcription initiation sites and function in maintaining a more permissive chromatin structure which allows regulation of gene expression. In the main CpG island are non-methylated promoting genes to be freely expressed. Nevertheless, aberrant CpG island methylation has been associated with various types of cancers. This aberration can include different mechanisms to induce gene silencing by either inhibiting or activating the recruitment of regulatory proteins such as transcription factors to DNA (Kanwal & Gupta, 2012).

Hypermethylated genes in cancers include tumor suppressor genes such as Rb promoter in retinoblastoma, MLH1 and PTEN in colorectal cancer, BRCA1 in breast cancer and ovarian cancer and MGMT in glioblastoma (Nagarajan & Costello, 2009; Virani, et al., 2013). Other genes include genes involved in DNA repair, cell cycle control and apoptosis (Sharma, et al., 2010).

Gene function	Genes
DNA repair	hMLH1 (mismatch repair gene 1) MGMT (O6-methylguanine–DNA methyltransferase), WRN (Werner syndrome, RecQ helikase like), BRCA1 (breast cancer 1)]
Cell cycle control	(p16 INK4a, p15 I NK4b, RB), Ras signaling {RASSF1A [Ras association (RalGDS/AF-6) domain family member 1],
Apoptosis	TMS1 (target of methylation-induced silencing 1), DAPK1 (deathassociated protein kinase), WIF-1, SFRP1]
Metastasis	cadherin 1 (CDH1), CDH13, PCDH10], KISS-1, E-cadherin
Tumor suppressor	RB, TP53
Angiogensis	THBS1, VHL
cell death resistance	Caspases, p14, DAPK

Table (3): Genes with hypermethylated promoter associated with cancer (How Kit, Nielsen, & Tost, 2012; Sharma, et al., 2010).

DNA methylation pattern is used as a biomarker for early diagnosis, prognosis and following up patients. The methylation pattern is tested using array or sequencing based techniques. Some promising biomarkers include CDKN2A and RASSF1A in breast cancer, CDKN2A, MGMT, MLH1 in colorectal tumors, CDKN2A in lung cancer and GSTP1, RASSF1A, APC in prostate cancer (How Kit, Nielsen, & Tost, 2012; Sharma, et al., 2010).

.

1.4 Brain tumors:

Brain tumors are the most common pediatric solid tumor and the second most common childhood malignancy after leukemia representing 22% of all malignancies up to the age of 14 and 10% of malignancies in the age group from 15 to 19 years old (Hasselblatt, et al., 2009). The incidence rate in Egypt is 16.9 per million per year in children less than 15 years old (El-Gaidi, 2011). Advances in surgical intervention, chemotherapy and radiotherapy resulted in a humble survival improvement. Molecular characterization and deep investigation of underlying genetic drivers of different pediatric brain tumor are essential to overcome poor therapeutic outcome and dismal survival rates.

1.4.1 Classification of primary pediatric brain tumors:

Brain tumors were historically classified according to their anatomic location in the brain into: brain stem, hemispheric, diencephalic, cerebellar and optic regions tumors (Patel & Tse, 2004). This classification system is no longer commonly used. Zulch was the first to attempt a histology based classification in 1979. Zulch's classification was revised several times with the advancement of immunohistochemistry and genetic profiling (Patel & Tse, 2004). Nevertheless, the original classification based on the anatomic location of the brain tumors is still being used in radiological investigation. Accordingly the four main groups are:

-Infratentorial including medulloblastoma, cerebellar astrocytomas, atypical teratoid/rhabdoid tumors and choroid plexus carcinoma.

-Supratentorial tumors including low-grade cerebral hemispheric astrocytomas, high-grade or malignant astrocytomas, primitive neuroectodermal tumors (PNETs), ependymomas, atypical teratoid/rhabdoid tumors and choroid plexus carcinoma.

-Parasellar tumors include craniopharyngiomas and germ cell tumors.

-Spinal cord tumors include gangliogliomas, ependymomas, low-grade cerebral hemispheric astrocytomas and high-grade or malignant astrocytomas.

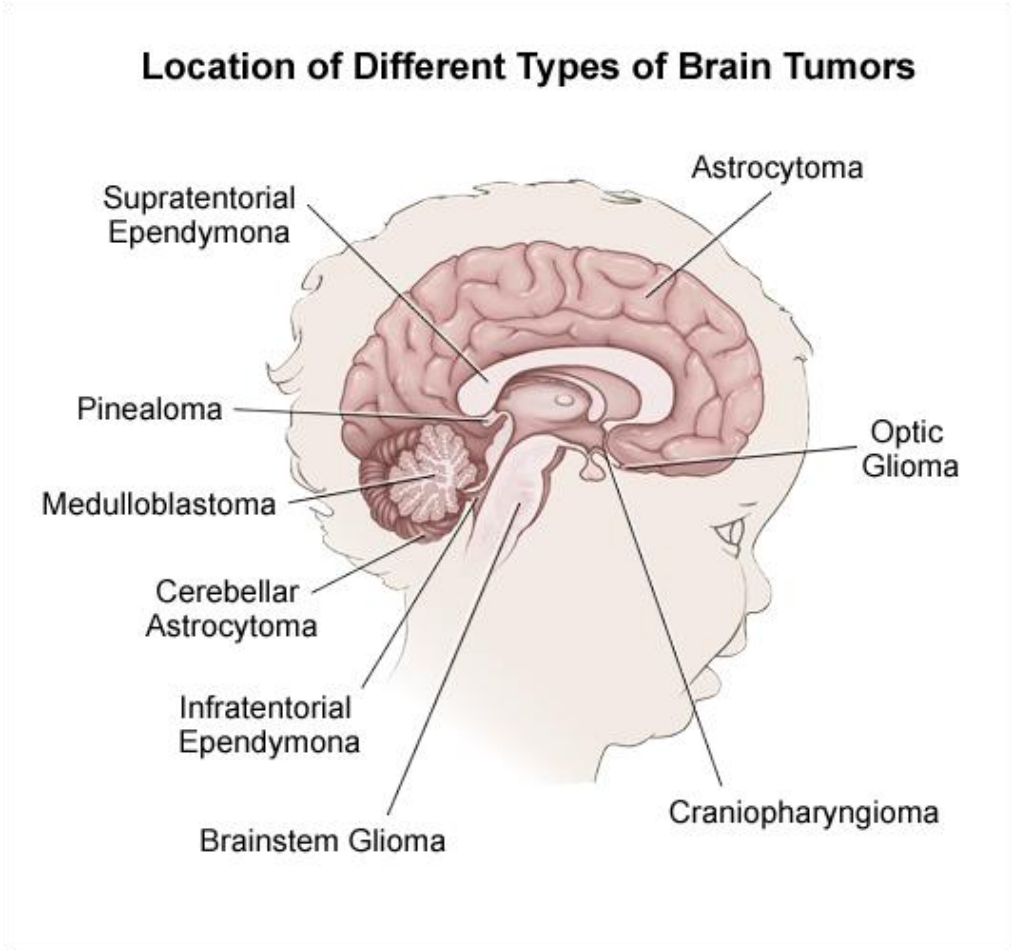

Figure (2): Morphological patterns of brain tumors showing the most common: astrocytoma, cerebellar astrocytoma, infratentorial ependymona, brain stem glioma, craniopharyngioma, optic glioma and medulloblastoma, www.hopkinsmedecine.org.

Currently the most commonly used classification is the World Health Organization (WHO) pediatric brain tumors classification which is based on the cell of origin which includes:

- Gliomas for cells of glial origin including: astrocytomas and ependymoma.
- Primitive neuroectodermal tumor (PNET) including medulloblastoma and supratentorial PNET
- Germ cell tumors including: germinoma .
- Other brain tumors are classified in miscellaneous group due to different cells of origin this group includes: craniopharyngioma, meningioma, hemangiopericytoma, hemangioblastoma and choroid plexus tumors (Paulino, 2011).

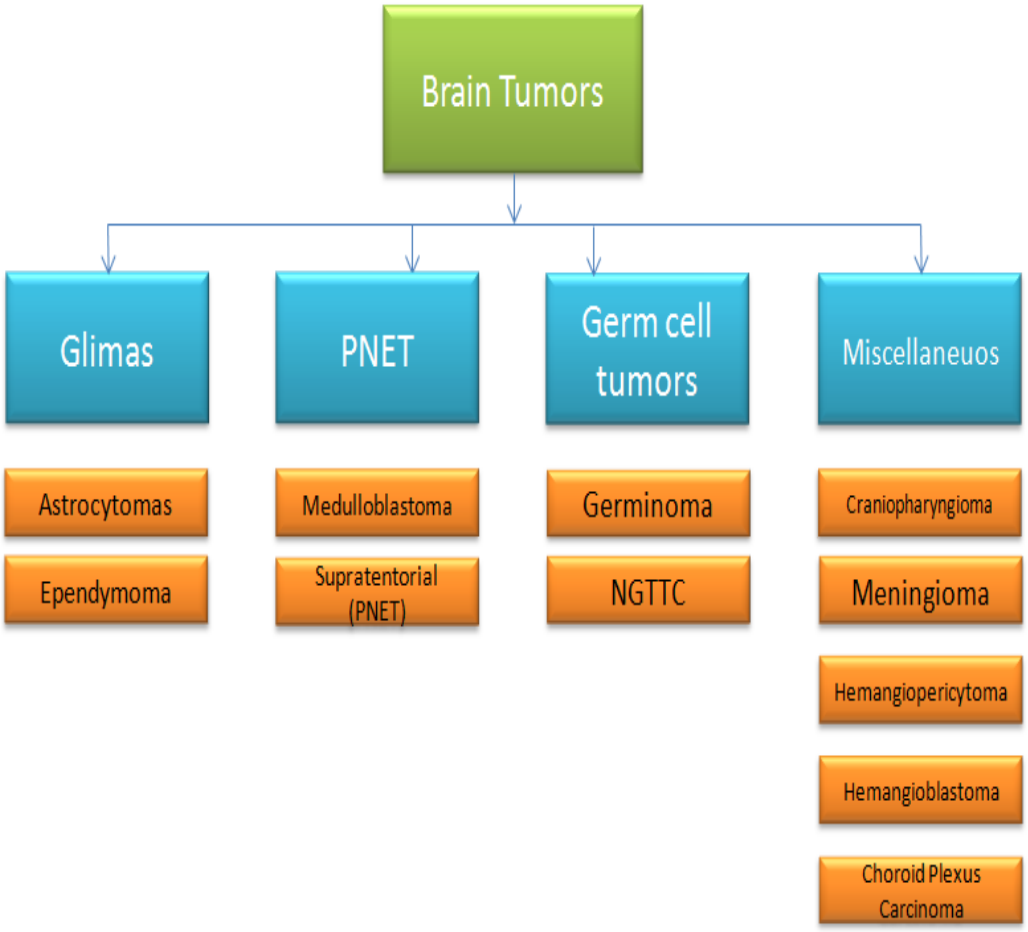

Figure (3): Classification of pediatric brain tumors according to cell of origin with 4 main subtypes: gliomas, PNET, germ cell tumors and miscellaneous (Paulino, 2011).

Cell or origin	Pediatric Brain tumor
Glioma	**Astrocytoma**: -Glioblastoma multiforme (WHO grade IV) -Anaplastic astrocytoma (WHO grade III) -Pleomorphic xanthoastrocytomas (WHO grade II) -Fibrillary astrocytomas (WHO grade II) -Juvenile pilocytic astrocytoma (JPA) (WHO grade I)
	Ependymoma: -Anaplastic ependymoma (WHO grade III) -Classic ependymoma (WHO grade II) -Subependymoma (WHO grade I) Myxopapillary ependymoma (WHO grade I)
	Other -Oligodendroglioma
Primitiveneuroectodermal tumors(PNET)	Medulloblastoma: the most common PNET
	Supratentorial PNET
Germ cell tumor	Germinoma
	NGGTC
Miscellaneous	-Choroid Plexus tumor -Craniopharyngioma -Hemangiopericytoma -Meningioma -Hemangioblastoma

Table (4): Classification of pediatric brain tumors according to cell of origin (Paulino, 2011).

1.4.2 CBRTUS distribution statistics of pediatric brain tumors:

The Central Brain Tumor Registry of the United States (CBTRUS) is the most comprehensive data bank in the united states of all the primary brain and central nervous system (CNS) tumors (http://www.cbtrus.org/, 2013).

The distribution of brain tumors according to CBRTUS in children aged 0-19 show the highest percentage of pediatric brain tumors in the frontal, parietal, temporal, and occipital brain lobes representing 16.9% of childhood tumors. Figure 4 shows the distribution of childhood tumors by site. Unlike the adults counterparts, the most common pediatric brain tumor is pilocytic astrocytoma followed by medulloblastoma (Morales & Gaskill-Shipley, 2010).

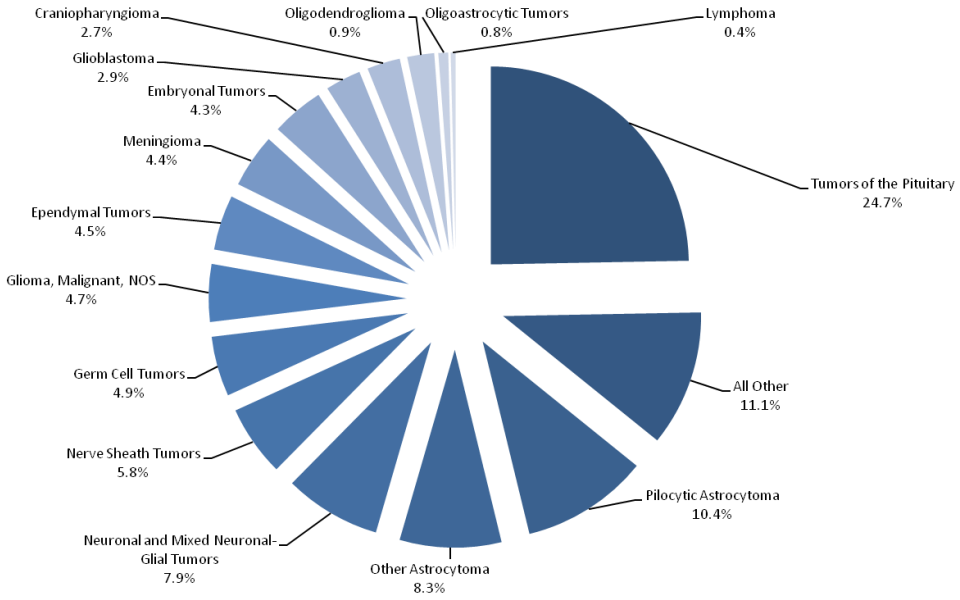

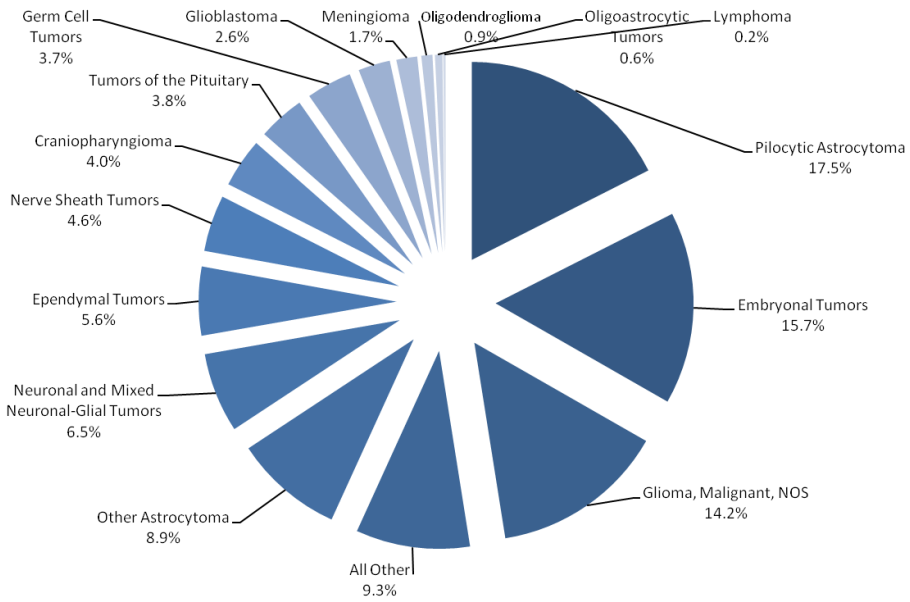

Figure (4): Distribution of childhood brain tumors according to CBRTUS by histology is shown in figure 4. (a) Represents the age group 0-14 and (b) represents the age group 14-19. http://www.cbtrus.org/

1.4.3 Genetic and non-genetic factors associated with childhood brain tumors:

Exposure to ionizing radiation and presence of familial genetic syndromes correlated with the development of childhood brain tumors (Fleming & Chi, 2012; Paulino, 2011). Exposure to ionizing radiation during radiotherapy on the central nervous system (CNS) predisposes to secondary meningioma and malignant glioma. Familial genetic syndromes represent around 5% of all childhood brain tumors. Examples of familial genetic syndromes are:

Neurofibromatosis Type 1 (NF1) which involves neurofibromin gene mutation on chromosome 17 resulting in mostly, optic pathway glioma.

Neurofibromatosis Type 2 (NF2) which is presented later in life than NF1 and is caused by a mutation on chromosome 22 for a gene responsible for Merlin protein transcription and resulting in acoustic neuroma.

Tuberous Sclerosis (TS*)* which is mainly associated with subependymal giant cell astrocytoma ependymoma and glioblastoma and was found to be linked to two genes TSC1 on chromosome 9 and TSC2 on chromosome 16.

Familial Cancer Predisposition Syndromes which involves mutation on tumor suppressor gene (*TP53*) on chromosome17 and increases the risk of several solid tumors including astrocytoma, glioblastoma and choroid plexus carcinoma.

Von Hippel Lindau which is caused by mutation on the *VHL* gene on chromosome 3 and is associated with Cerebellar hemangioblastoma pancreatic and kidney carcinoma.

Other hereditary syndromes include Gorlin's syndrome and Turcot's syndrome. It is of great importance for paediatricians who care for children of familial genetic syndrome to keep a close follow up and to thoroughly investigate all symptoms.

1.4.4 Grading of childhood brain tumors:

Grading of childhood brain tumors based on the biological behavior of the neoplasm is a complicated procedure. It takes into consideration its proliferative power, nuclear changes, mitotic activity, invasiveness and necrosis (Louis, et al., 2007; Patel & Tse, 2004), based on which the choice of adjuvant therapy is done. The WHO sets a grading scale from (I) to (IV) where (I) being benign and (IV) being the most malignant. The WHO classification Grade I describes neoplasm of low proliferative activity and good prognosis, Grade II designates low proliferative infiltrative neoplasm, Grade III is for lesions which show malignant evidence and grade IV for malignant neoplasm with high mitotic activity (Louis, et al., 2007).

1.4.5 Diagnosis and treatment:

The new modalities used in brain tumors diagnosis are the computed tomography (CT) and magnetic resonance imaging (MRI). These modalities improved the accuracy of diagnosis compared to older modalities such as cerebral angiograms and pneumoencephalograms (Patel & Tse, 2004). The MRI using gadolinium is used in both initial diagnosis and postoperative assessment which is done usually 2 days post-surgical resection. MRI is able to detect the spread of tumor. Staging in brain tumors is not a common practice and mainly depends on tumor size and the location of the specimen taken, marginal specimen usually show invasiveness and proliferation while core specimen commonly shows necrosis. (Patel & Tse, 2004; Paulino, 2011).

Treatment of brain tumor like every other solid tumor involves 3 therapeutic approaches; the first step is surgical resection. Even though complete resection is one of the few indicators of good prognosis, the surgeon still has to weigh between complete excision and trying to avoid any insult to the brain and possible neurological loss. The second step is usually radiotherapy. This step is the foundation of treatment of pediatric brain tumors. However, risks of developing secondary brain tumors and /or brain injury resulting in growth impairment as a result of exposure to ionizing radiation are still present. Lastly chemotherapy can be both administrated prior to resection to minimize tumor size or after excision to ensure elimination of cancerous cells.

The treatment protocol is determined by a team of surgeons, oncologists and neurologists who take into consideration the type of the tumor, the stage and the adverse effect of the treatment approach. The future promises genetic and molecular targeting therapies with the increasing knowledge of the different molecular pathways. Ras/Raf/MAPK, PI3K/AKT/mTOR and sonic hedghog are three of the potential promising pathways (Packer, 2012).

1.5 Choroid plexus:

Choroid plexus are non-neuronal epithelial cells located in the ventricular part of the vertebral brain. The choroid plexus together with other cells such as the tanycytes of circumventricular organs constitute the brain-CSF-Blood barrier. The main role of the choroid plexus is cerebrospinal fluid (CSF) production through their access to the leaky vessels blood compartments. CSF provides the brain and the spinal cord with many components that are required for normal nervous system function. In addition, it protects the nervous system from toxins (Wolburg & Paulus, 2010).

Anatomically, the choroid plexus is composed of 4 parts; two of the choroid plexus are located in the lateral ventricles originating from the inner ventricular system forming an undulated leaf like structure. The third choroid plexus protrudes from the 3rd ventricle Finally, the 4th plexus is arises from caudal ventral part of the cerebellum (Strazielle & Ghersi-Egea, 2000).

1.5.1 Choroid plexus tumors:

Choroid plexus tumors are rare neoplasms of the central nervous system. Although, they have glial origin they are classified separately from gliomas possibly due to their appearance which is characterized by papillary inter-ventricular growth. Fifty percent of CPT occur in the lateral ventricles, forty percent in the fourth ventricle and ten percent in the third ventricle or involve multiple ventricles (Gopal, Parker, Debski, & Parker, 2008; Wolburg & Paulus, 2010).

CPT accounts for 1% to 4% of all childhood brain tumors (Gopal, et al., 2008). They are more common in pediatric patients than in adults (Rickert & Paulus, 2001). Additionally, around 10% of CPT are choroid plexus carcinomas (Wolburg & Paulus, 2010).

Choroid plexus tumors are basically classified into three major groups: choroid plexus papilloma (CPP) which is according to the world health organization (WHO) is a grade I tumor. CPP represents 80 to 90% of CPTs, they show good prognosis with gross surgical resection. The atypical choroid plexus papilloma (ACPP) and choroid plexus carcinoma (CPC) represent a smaller percentage of the CPT than CPP (Gopal, et al., 2008; Wolburg & Paulus, 2010). CPCs is an aggressive malignant tumor (WHO grade III) represents around 10-20% of CPTs within the age group of 26 to 32 months old (Gopal, et al., 2008). CPCs have dismal prognosis which necessitate adjuvant treatment approaches. The tumor mainly involves the lateral and fourth ventricles (Kamaly-Asl, Shams, & Taylor, 2006). CPC is distinguished from CPP through their increased mitotic figures, nuclear to cytoplasm ratio and presence of necrosis (Hasselblatt, et al., 2006). All CPTs express vimentin, cytokeratin. Gene expression profiles identified more than 50 genes with different expression pattern found in CPC that distinguish it from CPP and ACPP (Hasselblatt, et al., 2006; Louis DN, 2007).

CPC is presented by increased intracranial pressure due to obstruction and overproduction of CSF. This results in many symptoms which include hydrocephalus, seizures, vomiting, headache, bulging fontanels and visual disturbance (Gopal, et al., 2008).

In order to improve patients' prognosis, complete gross resection of the tumor is necessary. Unfortunately, total resection is linked to higher morbidity due to the tendency of the tumor

to disseminate through the blood. Two thirds of the CPC tumors metastasize through the CSF. For the meantime, adjuvant chemotherapy and radiotherapy treatments remain controversial (Gopal, et al., 2008; Wolburg & Paulus, 2010). Recent studies were focused on using molecular targeting as treatment alternative in choroid plexus carcinoma. One study investigated targeting the platelet-derived growth factor receptor (PDGFR) beta using tyrosine kinase inhibitors. The inhibitor revealed attenuation in the proliferative activity of the tumor (Koos, et al., 2009). Moreover, another study conducted in the same year on the methylation pattern of the MGMT (O6- methylguanine-DNA methyltransferase) on choroid plexus carcinoma. The MGMT promoter revealed a methylation signal in 58% of the tumors investigated, suggesting a promising role for alkylating agents such as temozolomide in patients' treatment (Hasselblatt, et al., 2009).

1.5.2 Genetics of CPCs:

Brain tumors, similar to most cancer types could develop for multiple reasons; hereditary, chemicals, radiation and viruses. One of the most common dysfunctions involved in CPC formation is related to the tumor suppressor p53, more commonly found in families with Li-Fraumeni Syndrome (LFS) (Custodio et al., 2011). Recently, it was reported that fifty percent of the patients with choroid plexus carcinoma tested positive for germ-line TP53 mutations (Tabori et al., 2010). Furthermore, somatic mutations in TP53 have been identified in CPC patients (Tabori et al., 2010). Various chromosomal imbalances have been reported in studies of comparative genomic hybridization of CPTs. The following chromosomal additions and deletions have been displayed in patients with CPP: +12p; +12q, and +20p; +1, +4q, and +20q; +4p; +8q and +14q; +7q, +9p, and +21; -22q; -5q; -5p and -18q (Rickert et al., 2002). Certain imbalances were found to characterize of the type of tumor and the age of the patient at the time of the clinical presentation (Rickert et al., 2002).

1.6 Protein folding and quality control pathways:

The role of quality control pathways in protecting against misfolded and aberrant proteins has been under focus due to its relevance to many human cancers and neurodegenerative diseases. For the purpose of the work described in the thesis, protein folding and quality control pathways in eukaryotes will be discussed thoroughly. Protein folding is a process by which a polypeptide chain is converted to a functional three dimensional protein molecule

(Roman & Gonzalez Flecha, 2014). The process requires the assistance of multiple chaperons. As any other machinery folding may encounter several obstacles. These problems result in misfolded proteins (Garcia-Mata, Gao, & Sztul, 2002). Thirty percent of newly nascent polypeptide ends up being misfolded. Misfolding may be a result of errors in transcription, translation or due to environmental factors causing thermal, oxidative or osmotic stress. Such misfolded proteins may be refolded or eliminated using quality control mechanisms (Garcia-Mata, et al., 2002; Yao, 2010).

1.7 Quality control pathways:

Cell maintains the proteome homeostasis through balancing *de novo* protein synthesis and aberrant or misfolded protein degradation. The process of protein transcription and translation are extensively covered through many studies. On the other hand, protein degradation has not received the same attention until the beginning of the year 1940 (Lilienbaum, 2013). The process of protein degradation is governed by three major different yet interconnected pathways (Lilienbaum, 2013; Yao, 2010):

- First, the molecular chaperone pathway uses heat shock proteins (HSPs) to help efficient refolding of misfolded proteins.
- Second, the Ubiquitin Proteasome System (UPS) which is responsible for eradication of the majority of damaged, denatured and misfolded proteins.

-Third, the autophagy system which is an alternative pathway for elimination of abnormal protein aggregates.

The UPS and the autophagy pathways play a key role in energy production during starvation in addition to their role as quality control machinery.

1.7.1 The ubiquitin proteasome pathway:

The process of intracellular misfolded protein elimination is initiated by covalent attachment of one ubiquitin (Ub) molecule to a lysine residue on the protein to be degraded (Lilienbaum, 2013). Ubiquitin protein is a conserve 76 amino acid polypeptide which possess 7 lysine residues for subsequent ubiquitin bonding in a process known as poly ubiquitination (Hershko & Ciechanover, 1998) The process is activated by the successive activity of three enzymes : ubiquitin activating enzyme (E1), ubiquitin-conjugating enzyme (E2) and ubiquitin ligase (E3). The action is done through energy release from ATP (Lilienbaum, 2013). Depending on the length and positioning of ubiquitin moieties, different cell machinery are

recruited for degradation. The most abundant form is lysine 48 Ub which act as a signal for 26S proteasome degradation (Kravtsova-Ivantsiv & Ciechanover, 2012). The barrel shaped 26S proteasome has a channel structure through which the polyubiquinated misfolded protein gets degraded by specific enzymes (Groll & Huber, 2003). On the other hand, lysine 63 Ub has been recently associated with being a signal for non-proteasomal pathway including identification by aggresomes and autophagy pathway (Lilienbaum, 2013).

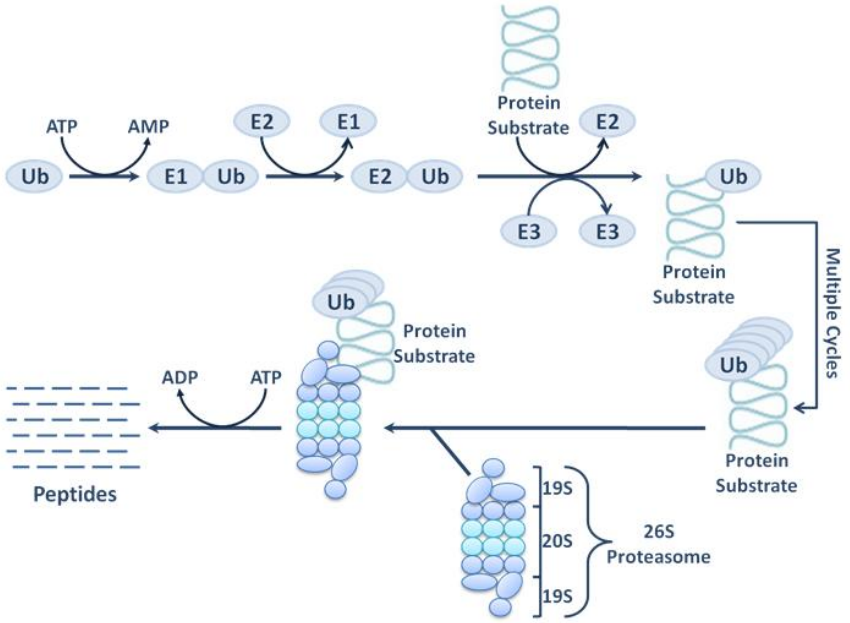

Figure (5): Schematic illustration of the ubiquitin proteasome pathway. The process is activated by the successive activity of 3 enzymes E1, E2 and E3; the barrel shaped 26S proteasome has a channel structure through which the polyubiquinated misfolded protein gets degraded by specific enzymes (Kinayamu, Chen, & Archur, 2005).

1.7.2 Autophagy:

Autophagy is a dynamic catabolic multistep process for elimination of toxic and misfolded proteins. The process is essential for cell protection against many diseases including cancers, infectious diseases, neurodegenerative and myodegenerative diseases (Loos, Engelbrecht, Lockshin, Klionsky, & Zakeri, 2013).

Autophagy is a Greek term which means “self -eating”. The cell recycles cytosolic components to be able to survive in stress conditions. There are three main types of

autophagy: macroautophagy, microautophagy, and chaperone mediated autophagy (CMA). Each type of autophagy has a different function and pathway. The most characteristic is macroautophagy which will be referred to as autophagy in the remaining part of the literature (Chen & Klionsky, 2011).

1.7.3 Macroautophagy pathway:

Autophagy is an essential catabolic process necessary to homeostasis inside the cell. It is mainly upregulated in cases of nutrient starvation, oncogene activation, infections and hypoxia (Rosenfeldt & Ryan, 2011). The process starts by formation of a crescent shaped sequestering double membrane compartment containing cell materials to be degraded, known as phagophore. The phagophore then elongates into autophagosome which subsequently fuses with the lysosome forming an autolysosome structure for subsequent degradation (Klionsky, et al., 2008).

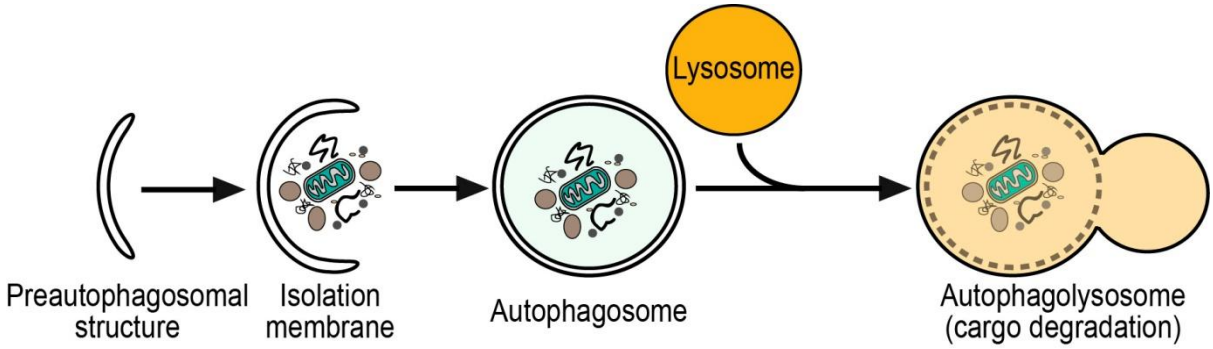

Figure (6): Schematic illustration of the macroautophagy pathway. The process starts by phagophore formation followed by elongation into autophagosome. The autophagosome then fuses with the lysosome releasing hydrolases for protein degradation (Grasso, Ropolo, & Vaccaro, 2015).

The machinery of autophagy is operated by a number of compounds which facilitate the fusion of the autophagosome with the lysosomes forming the autolysosmes, where toxic proteins are degraded. The process is initiated by the nucleation of the phagophore with the help of the autophagy effector activity of LC3; the phagophore is then assembled in a

phagophore assembly site (PAS). This assembly is done under the control of class III phosphatidylinositol 3-kinases (PI3K) (Lilienbaum, 2013; Mizushima, Yoshimori, & Ohsumi, 2011). The phagophore is later expanded in an elongation step forming the mature autophagosome. Two ubiquitin like (Ubl) complexes involved in the process; the Atg12-Atg5 ubiquitin-like conjugation system and the Atg8 proteins (Johansen & Lamark, 2011). The mammalian ortholog of Atg8 are the LC3 variants: LC3A, LC3B, LC3C, GABARAP (γ-AminoButyrate acid receptor-associated protein), GABARAPL1 (GABARAP-Like protein) (Lilienbaum, 2013). At this step LC3-I is cleaved then lipidated to the LC3-II isoform, which is then, incorporated into the autophagosome. The LC3-II is one of the specific markers for autophagy (Chen & Klionsky, 2011). The autophagosome then fuses with lysosome forming autolysosome in the maturation step for subsequent degradation by specific hydrolases, The autophagic process is highly regulated machinery and its miss-regulation is linked to many diseases including cancers (Lilienbaum, 2013).

1.7.4 Diseases associated with impaired autophagy:

Genetic connection between autophagy and cancer has been reported in several studies. Tumor suppressor genes were found to activate autophagy. On the other hand, oncogenes were linked to autophagy inhibition (Todde, Veenhuis, & van der Klei, 2009). In addition to their ambiguous role in cancers, perturbed autophagy was found to contribute to various diseases including neurodegenerative, cardiovascular and inflammatory diseases. Many autophagy genes were found inactivated in human cancers (Klionsky, et al., 2008; Rosenfeldt & Ryan, 2011; Sarkar, et al., 2013).

The autopahgy related gene, ATG Beclin1 hemizygosity was detected in a high percentage in human breast, ovarian and prostate cancers. Alternatively, the ectopic gene transfer was found to inhibit tumor growth in mouse and human xenograft models (Levine & Kroemer, 2008; Rosenfeldt & Ryan, 2011; Todde, et al., 2009). UV radiation resistance-associated gene protein (UVRAG), ATG5 and ATG12 mutations were reported in colon and gastric cancer .The p62/SQSTM1 was found overly expressed in breast and lung cancer (Schmukler, Kloog, & Pinkas-Kramarski, 2014).

1.7.5 The role of LC3 in autophagy:

The microtubule-associated protein light chain 3 (LC3) is the mammalian homologue of yeast ATG8 that was first detected to localize to autophagosome in the year 2000 by Kabeya et al

using electron microscopy (Kabeya, et al., 2000). LC3 and LC3 tagged with GFP are the markers of choice to monitor the autophagic process either by Western blot, immunofluorescence or life imaging (Klionsky, et al., 2008).

The process of LC3 lipidation begins with the endopeptidaseATG4 which cleaves the LC3 exposing Carboxyl terminal glycine forming the LC3I. An E1-like enzyme (ATG 7) then activates the LC3I. Next, with the help of a second E2-like enzyme (ATG3) the conjugation of phosphatidylethanolamine (PE) moiety is catalyzed forming the lapidated LC3II (lc3-PE) (Chen & Klionsky, 2011; Tanida, Ueno, & Kominami, 2004).

1.7.6 LC3 gene and methylation:

The process of autophagy requires LC3 in the process of nucleation and elongation of phagophore. A recent study in 2012 (Bai, Inoue, Kawano, & Inazawa, 2012) classified human LC3 gene family into five members: LC3A variant1:V1, LC3A variant 2, LC3B, LC3B2 and LC3C.

LC3A-V1 and V2 differ in their transcriptional start site and their N-terminal amino acid sequence. On the other hand LC3B1 and LC3B2 has different locus and differ in only 1 amino acid. LC3B was always considered as the key player in autophagy. In the former study, they were able to prove that LC3B and LC3A-V1 play a major role in autophagy. Another interesting finding was the LC3A-V1 may have a tumor suppressive activity. Therefore, its inhibition may lead to carcinogenesis. Perturbations in autophagy genes on the genetic and epigenetic level were found to trigger cancer development. Epigenetic LC3A- V1 inactivation by DNA methylation was detected in many cancer cell lines. Restoration of LC3A-V1 protein by stable re-expression was found to inhibit tumor growth *in vivo* in oesophageal squamous cell carcinoma (ESCC) cell lines (Bai, Inoue, Kawano, & Inazawa, 2012).

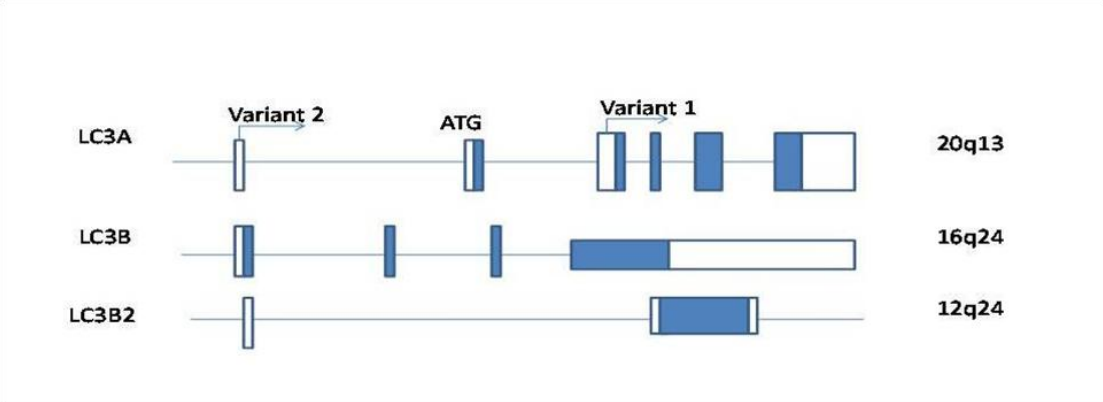

Figure (7): Human LC3 genes exon-intron structure, the diagram shows two variants for LC3A gene with 2 different transcriptional start sites (Bai, Inoue, Kawano, & Inazawa, 2012).

Cell lines with LC3Av1 silencing: 45.5% of all cell lines had LC3Av1 silenced while they all showed LC3B expression.

Cell line	Percentage LC3AV1 of silencing
Multiple myeloma	100%
Oral squamous cell carcinoma	83.3%
Endometrial carcinoma	80%
Esophageal squamous cell Carcinoma	66.7%
Hepatocellular carcinoma	61.1%
Thyroid cancer	50%
Ostesarcoma	50%
Gastric cancer	28.1%
Colorectal cancer	25%
Neuroblastoma	23.1%
Lung cancer	21.3%
Glioblastoma	9.1%

Table (5): Different cancer cell lines and the percentage of LC3Av1 silencing (Bai, Inoue, Kawano, & Inazawa, 2012).

.

1.8 Aggresome and autophagy:

Aggresomes are juxtanuclear protein aggregates which act as storage bins for misfolded proteins. They are localized in the microtubule organizing center (MTOC). Proteins sequestered in aggresomes are mainly cleared by autopagy (Yao, 2010).

The aggresomes were first identified by kopito lab in the year 2000. However, their exact composition is still not completely identified. Ubiquitin, Hsps 27, 70 and 90 and HDAC6 are key components in the aggresome structure (Richter-Landsberg & Leyk, 2013; Yao, 2010).

1.8 .1 Aggresome pathway:

When nascent polypeptide gets misfolded either due to failure in refolding or a dysfunction in the proteasome pathway, they aggregate to form aggresomal particles. These particles travel quickly towards the (MTOC) where they form the aggresome (1-3um) (Garcia-Mata, et al., 2002). This active process requires dynein/dynactin motor complex transport function and histone deactylase 6 (HDAC6) associations (Garcia-Mata, Bebok, Sorscher, & Sztul, 1999; Yao, 2010). The process is accompanied by reorganization of intermediate filament (IF) cytoskeleton protein vimentin forming a peri-centeriolar cage around the aggresome (Garcia-Mata, et al., 2002). Accumulation of toxic proteins in aggresome facilitates their degradation through autophagy (Lee, Shin, Choi, Lee, & Lee, 2002). This rescue machinery protects the cell from undesirable misfolded proteins and help in cell survival.

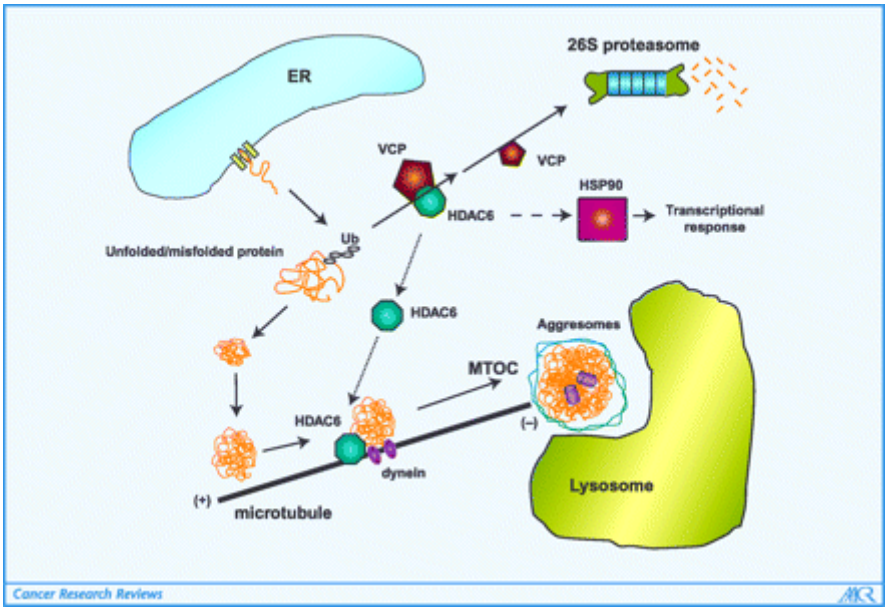

Figure (8): The aggresome pathway: misfolded proteins that don't get eliminated by the proteasomal system are transported by the help of HDAC6 and dynein motor to the MTOC region to be eliminated by autophagy (Rodriguez-Gonzalez, Lin, keda, Simms-Waldrip, et al., 2008).

Abnormal accumulation of poly-ubiquitinated misfolded protein aggregates has been reported in a number of neurodegenerative diseases including Alzheimer's disease (AD), Parkinson's disease (PD), Huntington's disease (HD), Lewybody dementia and amyotrophic lateral sclerosis (ALS) (Takalo, Salminen, Soininen, Hiltunen, & Haapasalo, 2013).

In Alzheimer's disease (AD) 2 different types of aggregates are reported: β amyloid peptide plaques found extracellular and the intracellular hyperphosphorylated tau proteins (Glenner & Wong, 1984; Kosik, Joachim, & Selkoe, 1986). In Parkinson disease (PD), accumulation of intracellular aggregates of synuclein in Lewy bodies is a common feature (Spillantini, et al., 1997). In Huntington's disease (HD) aggregates of polyglutamine (Poly-Q) extension containing Huntington protein are characteristic for the disease (DiFiglia, et al., 1997). Super oxide dismutase (SOD) aggregates in amyotrophic lateral sclerosis (ALS) are found in motor neurons (Bruijn, et al., 1998).

Inclusion body formation is a healthy mechanism for cell protection, however when their accumulation exceeds ability of quality control pathways to degrade the misfolded proteins they may target different compartments depending on their ubiquitination status and solubility. In Addition to the aggresome as compartment for insoluble ubiquitinated proteins,

they transport the misfolded protein for clearance by autophagy at the MTOC. Two different types of compartments where reported as targets for aggregated proteins:

-The Juxtanuclear quality control (JUNQ) which is a destination for soluble ubiquinated misfolded proteins. The aggregated proteins are either refolded or degraded using proteasome. The JUNQ is located in close proximity to the nucleus (Kaganovich, Kopito, & Frydman, 2008).

The insoluble protein deposit (IPOD) is non-membrane bound. The IPOD recruits the autophagy machinery for the disposal of insoluble non ubiquitinated aggregates such as in Huntington disease polyQ Huntington protein and prions (Kaganovich, et al., 2008). Compartmentalization of inclusion bodies and misfolded protein decrease their toxicity, improve their refolding through chaperon aid and boost the clearance process by proteasome or autophagy preventing their cross reaction with other active proteins.

1.9 Cross talk between UPS and autophagy

The aggresome/autophagy and the UPS pathways were long thought to be independent. Recent studies have shown several areas of crosstalk and complementation between both pathways in order to maintain homeostasis inside the cell. First level of interaction depends on the nature of protein to be degraded. Most short lived proteins favor degradation through the UPS system. Alternatively, long lived proteins and in case of proteasome overloading, misfolded proteins tend to form aggresomes as substrate for autophagy (Lilienbaum, 2013).

Second level of cross talk identifies the ubiquitin tagging of the protein. The K48Ub tag favors degradation by 26S proteasome (Kravtsova-Ivantsiv & Ciechanover, 2012), while K63Ub is a substrate for aggresome autophagy pathway (Tan, et al., 2008).

Third level of interfacing is the adaptor molecules which get attached to ubiquitnated proteins such as p62/sequestome-1 (SQSTM1) and BRCA1 (NBR) both of which have higher affinity to the K63 chains thus, they help in recruiting autophagic and not the proteasomal machinery (Kirkin, Lamark, Johansen, & Dikic, 2009). Another key molecule is HDAC6 which has a ubiquitin binding domain at its C- terminal and plays a role in aggresomes formation and transferring both the autophagosomes and lysosomes to the MTOC. Perturbation in UPS was found to redirect ubiquitinated protein aggregates into aggresome formation and hence elimination by autophagy (Driscoll & Chowdhury, 2012). Synergetic inhibition of both proteasomal and autophagy pathways is currently under investigation as powerful anticancer therapy.

1.10 HDAC6 and inhibitors:

Histone deacetylases (HDACs) are a group of enzymes that deactylate histones lysine residues as opposed to the action of histone acetyl transferases (HATs). Histones acetylation and deactylation play a role in chromatin dynamics and regulation of gene expression (Simoes-Pires, et al., 2013). However, more than 50 non histone substrates have been identified as HDACs targets (Fischer, Sananbenesi, Mungenast, & Tsai, 2010). HDACs are classified into four main classes based on yeast HDAC homology. Class I, II and IV activity includes Zn dependent mechanism, while class II is a NAD+ dependent mechanism. Class I has four isoforms (HDAC1, 2, 3 and 8), class III has 7 isoforms while class I has only HDAC11 isoform. Class II has 2 subclasses and 6 isoforms from which HDAC6 is in class IIb (Yang, Zhang, Zhang, Zhang, & Xu, 2013). The class HDAC6 plays a major role in the process of elimination of aggresomes (Simoes-Pires, et al., 2013).

HDAC6 is a 1215 amino acid protein structure with 2 catalytic deactylase domains (DD1 and DD2), the catalytic deactylase domain DD2 was found to play a major role in tubulin deactylation (Finnin, et al., 1999; Yang, et al., 2013). In addition, a zinc finger UBD was found at the C-terminal to bind with high affinity to ubiquitinated proteins. A dynein binding domain (DBM) is also present to facilitate the transport of ubiquitinated proteins along the microtubules towards the MTOC. HDAC6 recruits an actin remodelling system which helps in F-actin network assembly. This network assembly controls autophagosome and lysosome assembly (HDAC6-P62). Recent studies showed that HDAC6-deficient cells are unable to form large aggresome hence, misfolded protein elimination is impaired (Richter-Landsberg & Leyk, 2013).

HDACs inhibitors have been considered as novel potent cancer therapies. Unlike HDAC inhibitors, tubacin doesn't affect whole histone acetylation or gene expression (Richter-Landsberg & Leyk, 2013). Instead, it increases α-tubulin acetylation and inhibits aggresome formation through its interference with HDAC6 /dynein interaction.

1.11 mTOR pathway, an overview:

The mammalian target of rapamycin (mTOR) is a highly conserved 289 kD a serine–threonine kinase. It plays a role in regulation of cell growth, proliferation, metabolism and survival (Abraham, 2001). The mTOR belongs to the phosphatidylinositol kinase-related

protein kinases family, and its activation was reported in many human cancers. Two distinct mTOR complexes exist. The mTOR complex1 (mTORC1) composed of mTOR, raptor, PRAS40 and mLST8/GbL. The mTORC1 plays a role in protein synthesis and cell cycle, angiogenesis and autophagy. This complex exhibits sensitivity to rapamycin (Kim & Sabatini, 2004; Zaytseva, Valentino, Gulhati, & Evers, 2012). Second, The mTOR complex 2 (mTORC2) is composed of mTOR, rictor, mSIN1, mLST8/GbL, protor-1 and PRR5. The mTORC2 function includes cell survival, proliferation and actin cytoskeleton organization. Phosphatidylinositol3-kinase (PI3K)/Akt pathway/mTOR pathway was found to be deregulated in various types of cancers (Laplante & Sabatini, 2009; Zaytseva, et al., 2012). Targeting this pathway is an attractive goal for anticancer therapy.

Growth factors are the main activators of mTOR pathway. Among these growth factors are epidermal growth factor, and insulin like growth factor. They bind to their respective receptors such as receptor tyrosine kinase (RTK) eventually, this activates downstream signals such as PI3K (Engelman, Luo, & Cantley, 2006).

PI3K phosphorylates lipid phosphatidyl inositol 4-5 bisphosphate (PIP2) to the active phosphatidyl inositol 3, 4, 5, trisphosphate (PIP3) (Frech, et al., 1997). In turn, PIP3 recruits PH containing domain AKT phosphoinositide-dependent kinase to the cell membrane in parallel to recruiting 3-phosphoinositidedependent protein kinase 1 (PDK1) which phosphorylates AKT at threonine 308 (Thr 308) residue (Yap, et al., 2008). Further phosphorylation of AKT C-terminal serine 473 (ser473) by mTORC2 is mandatory for full AKT activation (Hennessy, Smith, Ram, Lu, & Mills, 2005). mTORC1 phosphorylates downstream p70 S6 kinase 1 (S6K1) and eukaryotic initiation factor 4E-binding protein 1 (4E-BP1). Both targets play a role in translation initiation. In addition, p70s6 Kinase has a feedback role in PI3K/AKT pathway inhibition (Zaytseva, et al., 2012).

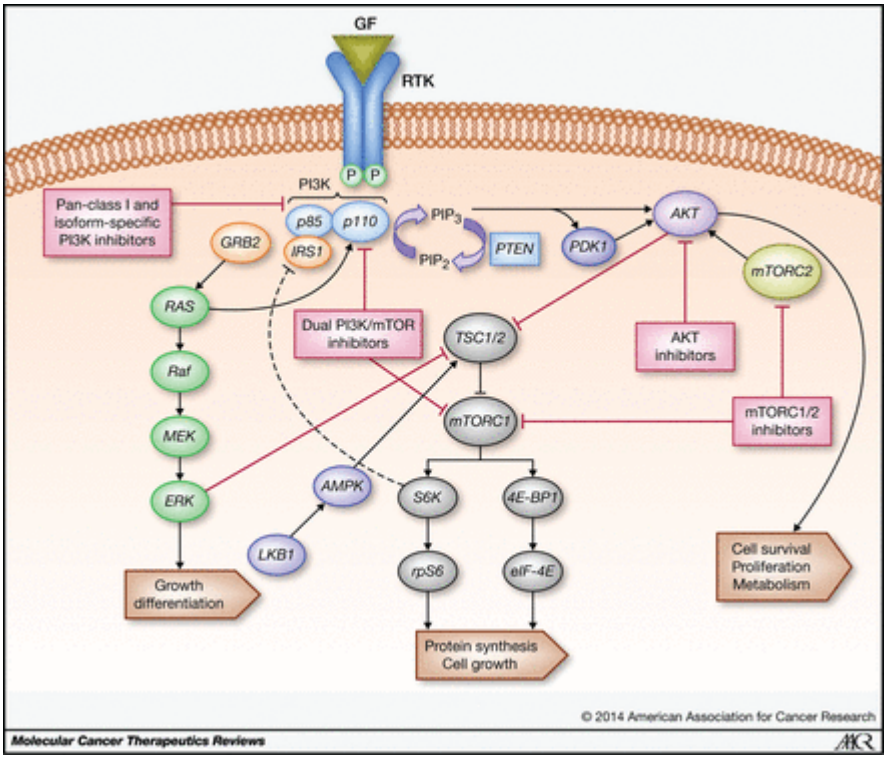

Figure (9): The mTOR pathway showing the activating nodes, AKT, PDK1, PI3K mTORC1 and mTORC2 and the negative feedback regulators PTEN and TSC complex (Dienstman, Rodon, Serra, & Tabernero, 2014).

Rapamycin and its analogs target mTOR inhibition through forming a complex with FKBP-12 which inhibits mTORC1 but not mTORC2 (Liu, Thoreen, Wang, Sabatini, & Gray, 2009). The drawback with rapamycin and its analogues that the S6K-mediated negative feedback loop is blocked by mtorc1 inhibition, leading to hyperactivation of PI3K signalling which in turn increases the phosphorylation of Akt -Ser473 and upregulates mTORC2 leading to further activation of AKT (Efeyan & Sabatini, 2010).

This limitation of rapamycin and its analogues lead to emergence of second generation mTORC1-mTORC2 dual inhibitors also known as ATP-competitive mTOR kinase inhibitors such as pp242, AZD, torin 1 and 2. Those inhibitors are able to block PI3K/Akt feedback signalling (Zaytseva, et al., 2012). In autophagy, the initial sequestration process is regulated by autophagy-related gene (Atg) products and mTOR proteins. mTOR pathway is activated by nutrients and growth factors which interacts with the cell membrane, starvation and lack of sufficient nutrients lead to mTOR inhibition and further activation of autophagy (Strimpakos, Karapanagiotou, Saif, & Syrigos, 2009).

Nutrients which enter the cell by passive diffusion activate mTORC1 through either direct interaction with mTORC1 or inhibition of tuberous sclerosis complex 1/2 (TSC1/2). Furthermore, low adenosine 5-triphosphate (ATP) production caused by energy deprivation causes activation of AMP dependent kinase (AMPK) deriving TSC1/2 activation hence, mTORC1 inhibition (Gao, et al., 2002).

2-MATERIALS AND METHODS

2.1-Specimen Collection:

Tumors diagnosis was carried out at the Department of Pathology, Children's Cancer Hospital Egypt 57357. Patients under 18 years of age diagnosed with choroid plexus carcinoma, papilloma or atypical choroid plexus papilloma with no prior exposure to radiotherapy or chemotherapy treatment were enrolled in the study. The study protocol was approved by the Children's Cancer Hospital Institutional Review Board (IRB). Informed consent was obtained from the patients or care-givers for the analysis of the stored samples (tissue) in this proposed study. Standard histological H&E preparations of the tumors were used to establish diagnosis for choroid plexus carcinoma and papilloma according to the WHO histological criteria.

2.2- Establishment of CCHE-45 Cell Line:

For the generation of the choroid plexus carcinoma cell line, half of the biopsy was paraffin embedded for histopathology and a small piece was further processed for culturing. For the generation of CCHE-45 cell line, tumor biopsy was initially minced and then cultured in RPMI media supplemented with 10% fetal bovine serum (FBS) and 5% antibiotics mixture of Streptomycin-penicillin-Amphotercin B (Lonza, Maryland, USA) at 37 ^{0}C and 5% $CO_{2.}$ Cells were regarded as immortal and stable after 40 passages, the cell line was established by Dr Shahenda El-Naggar lab team. CCHE-45 cell line was authenticated using Multiplex Cell Authentication by Multiplexion (Heidelberg, Germany). The SNP profiles for the cells and the tumor matched and were unique.

2.3- Karyotype and FISH Analysis:

Metaphase preparations were obtained from cell lines according to standard cytogenetics procedures. Giemsa staining and clonal chromosomal abnormalities were described according to the International System for Human Cytogenetic Nomenclature. FISH was performed on metaphase preparations from the same culture passage as conventional karyotyping. Whole chromosome paint and TP53/D17Z1 probes were used according to the manufacturer's instructions (Metasystems, Germany and Abbott, USA). The slides were analysed using Lieca DM5500 B microscope; subsequently image acquisition using JAI video camera and

image analyzer system (Applied Imaging Ltd) were used. The former experiments were conducted by cytogenetics team at Children Cancer Hospital Egypt 57357 under the supervision of Dr. Sherine Saleem.

2.4- Cell lines, Induction of Autophagy and Drug Treatment:

Neuroblastoma SH-SY5Y and SKNAS cell lines are a kind gift from Dr. Juma Mora at Sant Joan De Deu, Barcelona. Cells were authenticated using AmpFlSTR® SGM Plus® PCR Amplification Kit. Cells were grown in RPMI media containing 10% FBS and 1% antibiotics mixture of Streptomycin-penicillin-Amphotercin B (Lonza, Maryland, USA) at 37 ^{0}C and 5% CO_2. For induction of autophagy cells were serum starved in Hank's balanced salt solution (HBSS, Lonza, Maryland, USA) for 2 and 6 hours. For HDAC6 inhibition cells were treated with 15 μM tubacin or nil-tubacin (Enzo Life Sciences, New York, USA). For 5-AZA-dC treatment, cells were treated with either DMSO or 10 mM for 4 successive days (Sigma Aldrich, St Louis, Missouri, USA).

2.5- Western Blot Analysis:

Whole-cell lysates from both CCHE-45 and SH-SY5Y cell lines were prepared using RIPA lysis buffer (G-Biosciences, Missouri, USA) supplemented with protease and phosphatase inhibitors (ThermoScientific, Rockford, Illinois, USA). For Soluble and insoluble fraction protein isolation, cells were collected from 35 mm dishes and were lysed on ice for 30 min using 0.1% Triton X- PBS plus protease inhibitors (ThermoScientific, Rockford, Illinois, USA). Total cell extracts were centrifuged submitted 30 minute at 16,000 g to separate soluble (supernatant) and insoluble (pellet) fractions. The insoluble fraction was then resuspended in 1% SDS solution in 1X PBS. The proteins concentration was determined using Coomassie protein assay (Thermoscientific, Rockford, Illinois, USA). Protein lysate was resolved by SDS–PAGE (Bio-Rad, Berkely, California, USA) and blotted onto a PVDF membrane. After blocking with 5% non-fat dry milk in TBST for 1 hour, the membrane was incubated with primary antibody overnight at 4 ^{0}C.

The following primary antibodies were used with (1:1000) dilutions: rabbit anti-LC3A, rabbit anti-LC3B, mouse HDAC1, mouse ubiquitin, mouse anti-vimentin , mouse anti β-Actin (Cell Signalling Technology, Danvers, Massachusetts, USA) and mouse anti-acetylated alpha tubulin (Santa-Cruz Biotechnology, Santa Cruz, California, USA). The membrane was

washed 3 times with TBS each for 15 mins followed by secondary anti-mouse (1/5000) or anti-rabbit (1/5000) antibody for 1 hour. The membrane was then washed with TBS 3 times for 15 minutes each. Bounded antibodies were visualized using ECL chemiluminescence Western blot substrate (ThermoScientific Rockford, Illinois, USA).

2.6- Immunostaining and Immunofluorescence:

Automated immunostaining was carried out using Ventana BenchMarkXT platform using vimentin (Ventana,Tucson, Arizona, USA). The following antibodies were then used; vimentin, cytokeratin (Abcam, Cambridge, Massachusetts, USA), LC3A (Abgent, San Diego, California, USA) and LC3B. For immunofluorescence**,** cells were then fixed with 4% paraformaldehyde, washed with PBS, permeabilised and blocked in 5% normal goat serum and 0.2% Tween 20 at room temperature for 1h. Cells were then incubated at 37^0C with primary antibody overnight in humidified chamber, the following primary antibodies were used at the following concentrations rabbit anti-LC3A (1:50), rabbit anti-LC3B (1:50), mouse anti-vimentin (1:25), rabbit anti-HDAC6 (1:50) and mouse anti-acetylated α-tubulin (1:25). Cells were then washed with PBS and bound antibodies were visualized using the following secondary antibodies; Alexa Fluor 555 goat anti-mouse or Alexa Fluor 488 goat anti-rabbit antibody (1:500) (Cell Signaling Danvers, Massachusetts, USA) at room temperature for 1hour. After three further washes in PBS, cells were then counterstained using 4′, 6-diamidinophenylindole (DAPI). Images were acquired using LSM 710 confocal scanning laser microscope (Carl Zeiss, Thornwood, New York, USA).

2.7- Electron Microscopy:

Cell processing and EM imaging was performed at TEM Cairo University Research Park. In brief, cells were collected from plates using PBS then fixed with osmium tetroxide and glutaraldehyde, then dehydrated in different concentrations of alcohol and embedded in the selected epoxy resin. Microtome sections were then prepared at approximately 500 to 1000 µm of thickness with a Leica Ultracut ultramicrotome UCT (Leica Microsystems, Germany). Thin sections were stained with tolodin blue (1X). Ultrathin sections were prepared at approximately 75 to 90 of µm thickness and stained with lead citrate and uranyl acetate. Sections were examined using JEOL (JEM-1400 TEM) and captured by CCD camera AMT, optronics camera with 1632 x 1632 pixel format as side mount configuration.

2.8- Proteasome Activity Assay:

Three cell lines (CCHE-45, SH-SY5Y, SKNAS) were cultured overnight in a black wall transparent bottom 96 well plate. Cells were cultured at 500,000 cells/100ul/well at 37^{O}C and 5%CO2. The next day 100 µl of proteosome assay loading solution (Abcam, Cambridge, Massachusetts, USA) were applied and incubated at 37 ^{O}C for 4 hours and read at EX/EM 490/620 nm.

2.9- Cell Viability Assay:

Cells were platted at density 3000 cells/ well on a 96 well plate for 24 hours prior to treatment. Cells were treated with, tubacin, niltubacin (Life Sciences, New York, USA) or DMSO. After 48 hours the cells were then treated WST-1 (Clonetech, Mountain View, California, USA) which measures cell proliferation for 4 hours. Absorbance was measured at 440 nm using a spectrophotometric microplate reader (Sunrise, Tecan, Männedorf, Switzerland). All experiments were performed at least three times. Error bars represent ± SEM. The absorbance values were normalized to the control values.

Cell proliferation percentage: average OD drug exposure/average OD control X 100

Drug	**Concentration**
Tubacin	50, 25, 12.5, 6.25, 3.125, 1.56, 0.781uM
Niltubacin	50, 25, 12.5, 6.25, 3.125, 1.56, 0.781uM

Table (6): Different concentrations used for cell viability assay.

2.10- RNA Isolation, cDNA Synthesis and RT-PCR:

RNA isolation was performed using TRizol Reagent (Invitrogen Life Technologies, Carlsbad, California, USA) according to manufacturer's instruction manual. After decanting the culture media from the wells, 1ml of TRIzol reagent was added to each well. This was followed by

incubation for two min at room temperature. Lysed cells were then collected and transferred to a chilled microcentrifuge tube on ice. For each 1 mL of TRizol reagent, 0.2 mL of chloroform was added. Tubes were then vigorously shaked by hand for 15 seconds. This step was followed by an incubation time of three min on ice. Tubes were centrifuged for 15 min at 12,000 × *g*/ 4°C. Tubes were then angled at 45° to remove the aqueous phase of the sample by pipetting the solution while avoiding the interphase and the organic layer. The aqueous phase was then placed in new tube on ice. 0.5 mL of isopropanol was added to the recovered supernatant and incubated on ice for 10 min the solution was then centrifuged at 12,000 × *g* for 15 min at 4°C. The supernatant was then removed leaving the RNA pellet at the bottom. To wash the pellet 1 mL of 75% ethanol were used per 1 mL of TRIzol reagent. Tubes were centrifuged at 7500 × *g* for 5 min at 4°C to discard the wash. The RNA pellet was left to dry in air for10 min .The RNA pellet was then dissolved in RNase-free water. To determine RNA concentration UV spectrophotometer (Beckman Coulter DU ® 700 Series) was used. 2 µl RNA were diluted to a total of 100 µl of distilled water and measured at λ260 and λ280, the following formula was used to determine the concentration.

RNA concentration (µg/µl) = [OD260 x (dilution factor) x 40]/1000

cDNA was synthesized using RevertAid First Strand cDNA Synthesis Kit (ThermoScientific, Rockford, Illinois, USA). The following concentrations were used: 1µl of oligo (dT) 18 primer, 1µg of RNA and 10 µl nuclease-free water. Samples were then briefly centrifuged and left incubated for 5 min at 65°C. After centrifugation, samples were placed on ice. These reagents were added in the following order; 4µl 5X Reaction Buffer, 2 µl 10 mM dNTP Mix, 1 µl RiboLock RNase Inhibitor 20 u/µl and 1 µl RevertAid M-MuLV Reverse Transcriptase (200 u/µl) to a total of 20 µl of volume. The sample was incubated at 42°C for 60 min followed by increasing the temperature to 70°C for 5 min to stop the reaction. Ten µl of PCR products were loaded on 2 % agarose gel then stained with ethidium bromide. The gel was then visualized using Gel Documentation System.

2.11-Polymerase Chain Reaction:

PCR was carried out using DreamTaq DNA Polymerase Master Mix (ThermoScientific, Rockford, Illinois, USA) using our designed primers LCA_V1_F, LCA_V1_R, LCA_V2_F, LCA_V2_R, LC3B_F and LC3B_R described in table 8.

Reaction Component	**Concentration**
DreamTaq DNA Polymerase Master Mix	25 µL
Forward primer	1 µL
Reverse primer	1 µL
Template DNA	5 µL
Water nuclease-free	18 µL
Total volume	50 µl

Table (7): PCR reaction components.

Primer	**Sequence**
LC3A-V1 forward	5'-CGTCCTGGACAAGACCAAGT-3'
LC3A-V1 reverse	5'-CTCGTCTTTCTCCTGCTCGT-3'
LC3A-V2 forward	5'-ACTCCTGACTGCATGGAAGC-3'
LC3A-V2 reverse	5'-GTCCACAGCTGCTTTTCCAC-3'
LC3B forward	5'-CGGAGAAGACCTTAAGCAG-3'
LC3B reverse	5'-TGACATGGTCAGGTACAAGGA-3'

Table (8): PCR primers for LC3 genes expression.

2.12-Bisulfite Sequencing:

2.12.1- Extraction of Genomic DNA:

DNA was extracted from CCHE-45 and SH-SY5Y cell lines using GeneJET Genomic DNA Purification Kit (ThermoScientific, Rockford, Illinois, USA), according to the manufacturer's protocol. Cells at 80% confluence were detached from the culture plate using Trypsin (Lonza, Walkersville, Maryland,USA). The Cells were then transferred in to a microcentrifuge tube to be pelleted by centrifugation at 1300 rpm x g for 5 min. To resuspend the cells 200 µl of PBS buffer were used (Lonza, Walkersville, Maryland, USA). Next, to lyse the cells 200 µl of lysis solution and 20 µl of Proteinase K solution were added. To obtain a uniform suspension Cells were pelleted then vortexed. Samples were left incubated at 56°C for 10 min with occasional vortexing until the cells were lysed completely. 400 µl of 50% ethanol was added to the lysed cells. The lysates were then transferred to GeneJET Genomic DNA Purification columns and centrifuged at 6000 xg for 1 min. The GeneJET purification columns were then placed into a collection tube. 500 µl of wash buffer I was then added and centrifuged for one min at 8000 xg. This step was followed with wash buffer II and centrifugation for 3 min at (≥12000 x g) which is the maximum speed. The genomic DNA was then eluted with 50µl of elution buffer. The elution buffer was added to the center of the GeneJET Genomic DNA purification column membranes for complete to elution of the genomic DNA. Finally, an incubation period of 2 min for the samples at room temperature followed by centrifugation for 1 min at 8000 xg. Isolated genomic DNA was stored at -20°C. The total DNA concentration was measured using UV spectrophotometer (Beckman Coulter DU ® 700 Series). 2 µl of genomic DNA were diluted to a total of 100 µl of distilled water and measured at λ260 and λ280. To determine the final concentration in µg/µl the following formula was then used.

DNA concentration (µg/µl) = [OD260 x (dilution factor) x 50]/1000

2.12.2- Bisulfite Treatment of DNA:

Two µg of DNA were used for bisulfite DNA modification using EpiTect Bisulfite DNA conversion kit (Qiagen, Hilden, Germany) according to the manufacturer's protocol. The total number of aliquots of the bisulfite mix was then dissolved in 800 µl RNase-free water. The aliquots were then vortexed until the bisulfite mix was completely dissolved. The bisulfite reactions were prepared as follows:

Reaction Component	Concentration
DNA solution	2ng
RNase-free water	To a total of 140 µl
Bisulfite Mix	85 µl
DNA Protect Buffer	35 µl
Total volume	140 µl

Table (9): Bisulfite reaction master mix components.

The bisulfite DNA conversion was performed using the following conditions:
Denaturation at 95°C for 5 min,
Incubation at 60°C for 25 min,
Denaturation at 95°C for 5 min,
Incubation at 60°C for 85 min,
Denaturation at 95°C for 5 min,
Incubation at 60°C for 175 min.
Finally Hold at 4°C.

2.12.3- Cleanup of Bisulfite Converted DNA:

Directly after the bisulfite conversion, the bisulfite reactions were centrifuged briefly, and then transferred to a new 2 ml microcentrifuge tubes. 550 µl of the freshly prepared buffer BL containing 10 µg/ml carrier RNA was added to each of the samples. The solutions were mixed by vortexing and then centrifuged briefly. The whole mixture was then transferred into

the EpiTect spin columns. Spin columns were then centrifuged at maximum speed (≥12000 x g) for one min. This was followed by discarding the flow-through. For the washing step, 500 µl Buffer BW was added to the spin columns and centrifuged at the maximum speed of (≥12000 x g) for one min and the flow-through was again discarded. For desulfonation, 500 µl Buffer BD was added to the spin columns and left incubated for 15 min at room temperature at (25°C). Centrifugation of the spin columns at maximum speed to discard the flow-through was done at maximum speed for 1 min. To each spin column 500 µl Buffer BW was added to the spin columns and centrifuged at for 1 min at maximum speed. The flow-through was then discarded. The washing step was repeated two times followed by centrifugation to remove any remaining liquid. Finally, 20 µl of the elution buffer (EB) were added to the center of each of the spin columns membrane to elute the DNA. The columns were then centrifuged for 1 min approximately at 15,000 x*g*.

2.12.4: Bisulfite Sequencing Primer Design:

Bisulfite-treated DNA was amplified using the designed bisulfite sequencing primers. Primers were designed using Methyl primer express® software v1.0 (Applied BioSystems, Life Technologies, Carlsbad, California, USA).

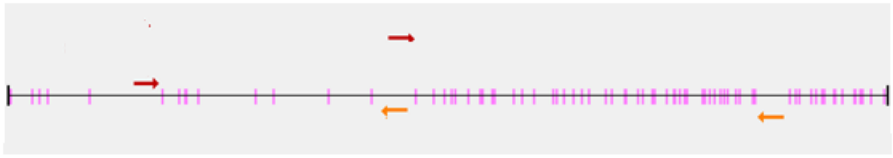

Figure (10): Schematic presentation of bisulfite sequencing primers.

Primer	**Sequence**
LC3A region1 Forward	5'-ATTTTTGGTAGTTTTTTTTTAGG-3'
LC3A region 1 Reverse	5'-ACAATCAAACACAAAATAAAACA-3'
LC3A region 2 Forward	5'-GTTTTATTTTGTGTTTGATTGTG-3'
LC3A region 2 Reverse	5'-TCACAACATTCCTTAAAAAAAA-3'

Table (10): Bisulfite sequencing primers.

2.12.5: Polymerase Chain Reaction:

As previously described.

2.12.6: Size Selection on Agarose:

Onto 1% agarose gel, 100 µl of sequencing PCR products were loaded followed by staining with ethidium bromide. The gel was then visualized. GeneJET Gel Extraction Kit (Thermo Scientific, Rockford, Illinois, USA) was used to extract the PCR product according the manufacturer's protocol. Using a clean scalpel, the gel containing the DNA fragment was excised and transferred into a 15 ml tube. The binding buffer was then added with the ratio 1 volume: 1 weight to the gel slices. The mixtures were then incubated at 60°C for another 10 min until the gel was completely dissolved. The dissolved gel solutions were transferred to the purification columns and centrifuged at max speed for 1 min. The columns were placed into the same collection tubes and the flow-through was discarded. 600 µl of the wash buffer were added to the GeneJET purification columns and centrifuged for another 1 min to fully remove any residual washing buffer. For elution, the GeneJET purification columns were placed into a new 1.5 ml microcentrifuge tubes and fifty µl of elution buffer were added to the centre of the column membranes. The tubes were then centrifuged for an additional 1 min and the DNA was kept under -80°c.

2.12.7-Tailing Reaction:

The tailing reaction was carried out using the non-proof reading Taq DNA Polymerase Recombinant enzyme (ThermoScientific, Rockford, Illinois, USA) as follows: The reaction mixture was incubated for 2 min at 70 ºC.

Reaction Component	Concentration
PCR product	20 µl
Taq Buffer with KCl (10X)	5 µl
25 mM $MgCl_2$	3 µl
Taq polymerase	1.25 µl
dATP (10mmol)	1 µl
Water	19.75 µl
Total volume	50 µl

Table (11): Tailing reaction components.

2.12.8-Purification:

Purification was carried out using PCR Purification Kit (ThermoScientific Rockford, Illinois, USA) according to manufacturer's protocol. To a ratio of 1:1 the tailing reaction was added to the binding buffer and transferred to the Gene JET purification columns. The columns were then centrifuged for 1 min .The flow-through was discarded, followed by the addition of 100 µl of Binding Buffer to the Gene JET purification columns and centrifuged for 1 min. The Gene JET purification columns were then transferred into a new 2 ml microcentrifuge tube. To elute, 25 µl of the elution buffer were added to the purification column membranes and followed by a centrifugation for 1 min.

2.12.9- Bisulfite PCR Cloning:

PCR products were cloned using InsTAclone PCR Cloning Kit (ThermoScientific, Rockford, Illinois, USA). The ligation reactions mixture were set as follows; 3 µl of 5X ligation buffer, 0.17 pmol vector pTZ57R/T, 6 µl of purified PCR, 1 µl T4 DNA Ligase giving a total volume of 30 µl. The Ligation mixtures were left incubated for 1 hour at room temperature (22°C). *E-Coli* JM109 competent cells (TaKaRa, Mountain view, California, USA) were left to thaw on an ice bath directly before use. 50 µl of thawed cells were mixed gently with 2.5 µl of each ligation mixture for bacterial transformation and kept on the ice bath for another 30 min.

Cells were then instantaneously heat shocked for 45 sec at 42 ºC and quickly returned to the ice bath for another 2 min. 500 µl of pre –incubated SOC medium at 37 ºC were added to the competent cells and left incubated while shaking (160-225 rpm) for another 1 hour at 37 ºC. SOC media containing transformed *E-Coli* were then placed on selective media containing 20 mg/ml X-Gal, 100 mM IPTG and 50 mg/ml ampicillin.

2.12.10- Plasmid Extraction:

Plasmid extraction was carried out using GeneJET Plasmid Miniprep Kit (ThermoScientific, Rockford, Illinois, USA) according to manufacturer's recommendation. Positive colonies were used to inoculate 5 ml of LB medium supplemented with the 50 mg/ml ampicillin antibiotic. Bacterial cultures were incubated while shaking at 200-250 rpm, overnight at 37°C. The cultures were then pelleted by centrifugation at 8000 rpm in a microcentrifuge for 2 min at room temperature. Harvested cells were resuspended in 250 µl of the resuspension solution. Cells were then transferred to a new microcentrifuge tubes. The lysis solution was then added to lyse the bacterial cells. The tubes were then inverted for 4-6 times to mix thoroughly until the solution became viscous and slightly clear. The tubes were then centrifuged for an additional 5 min to pellet the debris and DNA. The upper supernatants phase was then transferred to the spin columns by pipetting. Spin columns were centrifuged for another 1 min and discarded the flow-through. For washing, 500 µl of the wash solution were pipetted to the GeneJET spin columns and followed by centrifugation for 60 sec. This wash was repeated two times. Finally, 25 µl of the elution buffer were added to the of the purification column membranes and centrifuged for 1 min to elute the total plasmid DNA.

2.12.11- Colony PCR Identification:

The DNA was amplified using universal M13/pUC Sequencing Primers (Thermo Scientific, Rockford, Illinois, USA) using Dream Taq polymerase (Thermo Scientific, Rockford, Illinois, USA) the total reaction volume was 50 µl:

Reaction Component	Concentration
DreamTaq DNA Polymerase Master Mix	25 µL
Forward primer	1 µL
Reverse primer	1 µL
Template DNA	5 µL
Water nuclease-free	18 µL
Total volume	50 µl

Table (12): Colony PCR reaction components.

2.12.12- DNA Sequencing:

Sequencing was done in our lab using 3130 DNA Analyzer following the BigDye® Terminator v1.3 Cycle Sequencing protocol (Applied BioSystems, Life Technologies, Carlsbad, California, USA). Sequences from ten clones from each sample were then analyzed using BiQ Analyzer to identify methylated and unmethylated CG dinucleotides.

Reaction Component	Concentration
Terminator ready reaction mix	8ul
Template	Equivalent to 300 ng
Primer	3.2 pmol
H2O	Up to 20ul
Total volume	20ul

Table (13): Sequencing PCR reaction master mix components.

2.13- Cloning and Expression of LC3A Gene in Choroid Plexus Cell Line:

2.13.1- LC3A Amplification:

RNA and cDNA synthesis was done as mentioned above; LC3A-V1 and LC3A-V2 transcripts were amplified from SH-SY5Y and cells using primers LCA_V1_cDNA_F, LCA_V1_cDNA_R, LCA_V2_cDNA_F and LCA_V2_cDNA_R.

Primer Name	**Sequence**
LCA_V1_cDNA-F	5'-AAAAAGAATTCATGCCCTCAGACCGGCC-3'
LCA_V1_cDNA-R	5'-AAAAAGGATCCTCAGAAGCCAAGGTTTCC-3'
LCA_V2_cDNA-F	5'-AAAAAGAATTCATGAAGATGAGATTCTTCAGTT-3'
LCA_V2_cDNA_R	5'-AAAAAGGATCCTCAGAAGCCGAAGGTTTCC-3'

Table (14): LC3A-varient I and LC3A-varient II cloning primers.

50 µl of PCR products were loaded onto 1% agarose gels stained with ethidium bromide. The gel was visualized using Gel Documentation System. DNA was extracted using GeneJET Gel Extraction Kit K0691 (Thermo Scientific, Rockford, Illinois, USA) according to manufacturer's protocol as previously described.

2.13.2: Double Digestion:

Purified PCR product and p-IRES2-AcGFP Plasmid (Clonetech, Mountain View, California, USA), were double digested with *EcoR1* and *BamH1* restriction enzymes (ThermoScientific, Rockford, Illinois, USA) as follow:

Restriction enzymes master mix	**Concentration**
Water, nuclease free	Up to 20ul
10X Fast Digest buffer	2ul
Plasmid DNA(0.2ug)	Variable
FastDigest EcoR1	1ul
FastDigest BamH1	1ul

Table (15): Restriction master mix.

The reaction was mixed gently and incubated at 37°C for 5 min. This step was followed by a purification step using PCR Purification Kit (ThermoScientific, Rockford, Illinois, USA) as described earlier.

2.13.3: pIRES2-AcGFP Plasmid LC3A Insert Ligation:

The Vector – insert reaction mixture was prepared as follow:

Ligation Reaction Components	**Concentration**
Linear Vector DNA	20-100ng
Insert DNA	5:1
10X T4 DNA ligase buffer	2ul
T4 DNA ligase	1ul
Water, nuclease free	To 20ul

Table (16): p-IRES2-AcGFP Plasmid LC3A insert ligation mixture.

The reaction was incubated for 10 min at 22°C followed by transformation.

2.13.4-Transformation of Cloned Plasmid:

DH alpha Competent Cells (TaKaRa, Mountain View, California, USA) were thawed on ice bath just before use. Gently cells were mixed with 5 µl of the ligation mixture for bacterial transformation. Cells were then kept on ice for 30 min. This step was followed by a heat shock at 42° C for 45 sec, cells were then returned to ice for an additional 2 min. 500 µl of SOC medium pre-incubated at 37° C were added to the cells and left incubated while shaking at 225 rpm for 1 hour at 37° C. cells were then plated on kanamycin selective media. Plasmid preparation was then performed on selected colonies as previously described using GeneJET Plasmid Miniprep Kit (ThermoScientific, Rockford, Illinois, USA). Positive colonies were sequenced to confirm correct sequences for both variants to match LC3A-V1 (NM_032514.3) and LC3A-V2 (NM_181509.2).

2.13.5: Lipofectamine Transfection:

CCHE-45 Cells were cultured and left to reach 90% confluency, Lipofectamine 2000 (Life Technologies, Carlsbad, California, USA) was then diluted in serum free media, mixed with 2.5 ug of DNA (empty vector, LC3A-V1 or LC3A-V2) and incubated for 5 min at room temperature. The DNA-lipid complex was then added to the cells and incubated for 24, 48 or 72 hours.

2.14-BrainSpan Data Analysis:

Human BrainSpan project was used to obtain RPKM for the LC3A (ENSG00000101460) and LC3B (ENSG00000140941). Expression values were calculated for each gene according to developmental stage or across different brain regions. Analysis was performed using R statistical language version 3.2.2.

2.15-Statistical Analysis:

All experiments were repeated three times. Data are expressed as $\pm$ SEM. The significance of difference among means was evaluated using paired Test. Significant differences were defined as $p \leq 0.05$.

3-RESULTS

3-1: Constitutive formation of aggresomes in choroid plexus carcinoma line CCHE-45 is repressed by HDAC6 inhibitor.

We propagated a primary cell line, named CCHE-45, from a CPC surgical excision sample. Identity with the original tumor was verified using Multiplex Cell Authentication service (MCA), which utilizes a single-nucleotide polymorphism (SNP) profiling approach. Cells were passaged over forty times before considered immortal. Karyotyping was done in the pathology lab in children cancer hospital 57357.CCHE-45 cells presented with two clones, one clone was triploid (62~75 chromosomes) and the second clone was hexaploid (137 chromosomes). Structural abnormalities included translocation (2;18)(q32;q23), (1;3)(?;q27) and (20;22)(p11;q11) and del(17)(p11) (Figure 11) in both clones whereas the hexaploid clone had two copies from each translocation

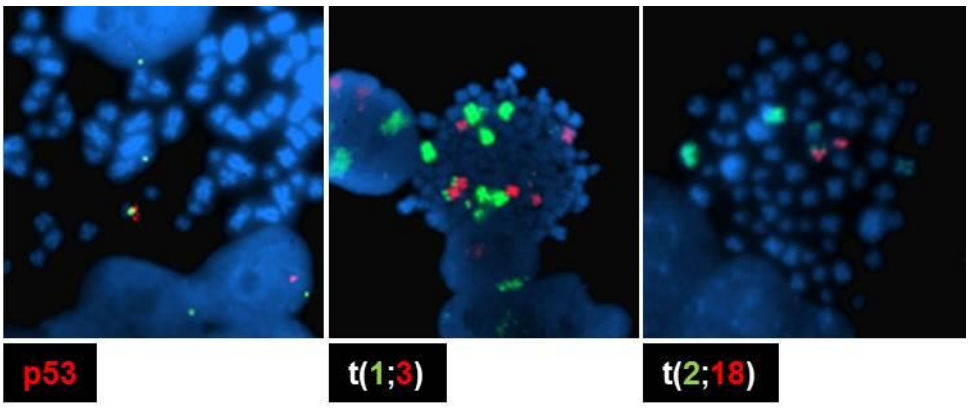

Figure 11: FISH analysis using red and green probes to detect *Tp53* gene and centromere, translocation t(1;3) and translocation t(2;18).

When immunostained with vimentin, a marker for choroid plexus tumors, CCHE-45 cells displayed a single perinuclear vimentin positive inclusion in all cells and in different passages (early and late); however, it varied in their intensity and size (Figure 12).

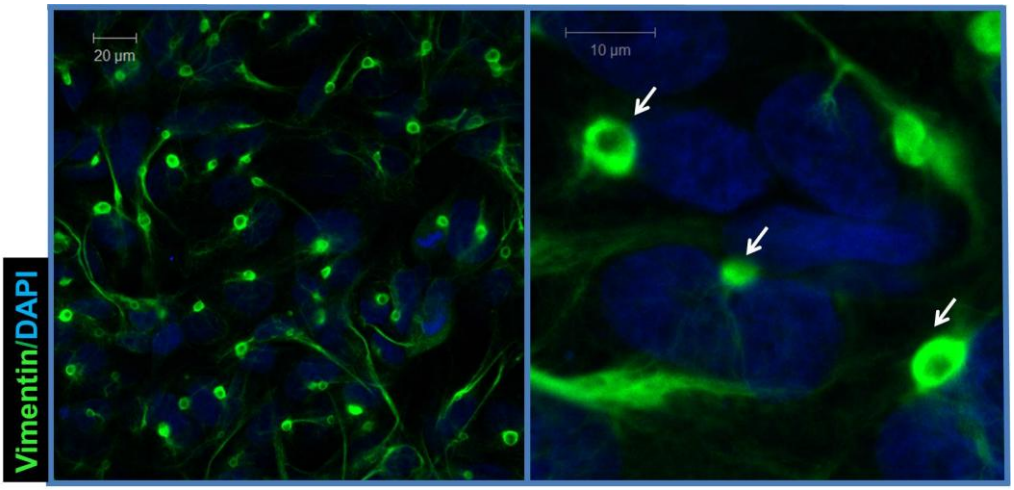

Figure 12: Aggresomes subcellular localization was identified by the formation of vimentin capsules (white arrows) at the MTOC. CCHE-45 cells were cultured under normal condition, fixed and immunostained with anti-vimentin (green) and visualized using Alexa Flour 488 anti-rabbit IgG antibody. Cells were counterstained with DAPI (blue) to visualize the nucleus.

The presence of vimentin cage like structures is characteristic of aggresomes and is formed by the collapse of the intermediate filament. Examination of CCHE-45 cells by transmission electron microscopy (TEM) further confirmed the presence of dense to light 2-3 µm in diameter perinuclear structures in most of the examined cells (Figure 13).

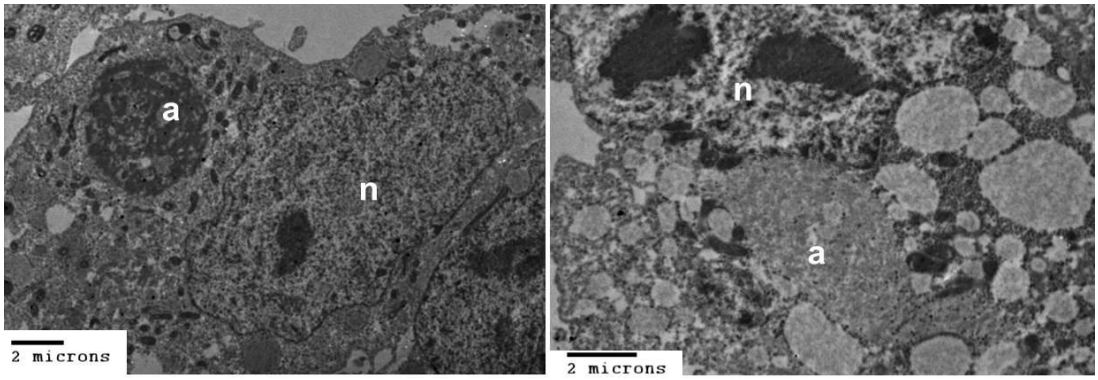

Figure 13: TEM examination of CCHE-45 cell line showing aggresomes ultra structures (a= aggresomes, n= nucleus).

These inclusion bodies varied in its density and in size. To ensure that the collapse of vimentin filaments was not a feature of the cell line and it is present in the original tumor, we examined a cell pellet from CCHE-45 cells and compared it to its original tumor tissue. Both CCHE-45 cells and the parent tumor displayed similar structures (Figures 14A and 14B). Unexpectedly, cytokeratin also contributed to the structure of aggresomes (Figures 14A and 14B).

A.

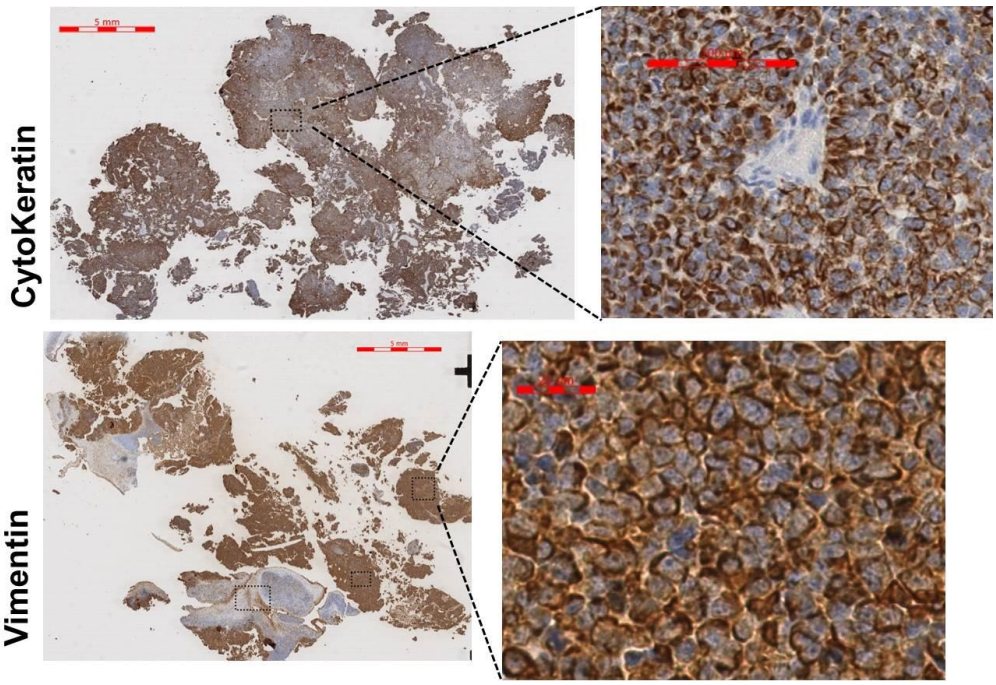

B.

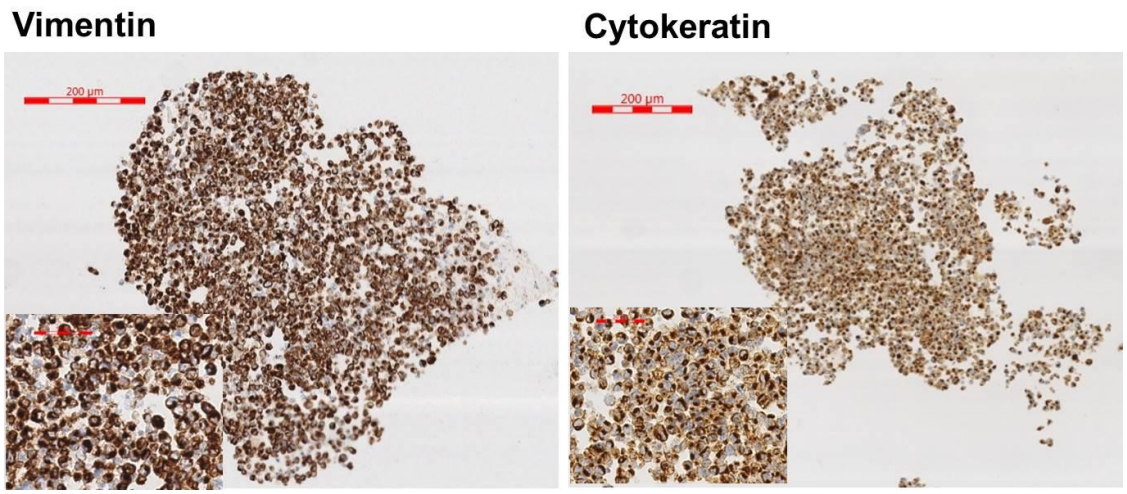

Figure 14:

A. CCHE-45 cell pellet was FFPE and immuno-stained with cytokeratin and vimentin.

B. CCHE-45 original tumor biopsy obtained at surgical resection was FFPE and immune-stained with cytokeratin and vimentin.

We further examined the pattern of vimentin and cytokeratin expression in CPP and ACPP. Both tumors displayed a homogenous cytoplasmic pattern for both markers suggesting that aggresomes are unique to CPC (Figure 14C).

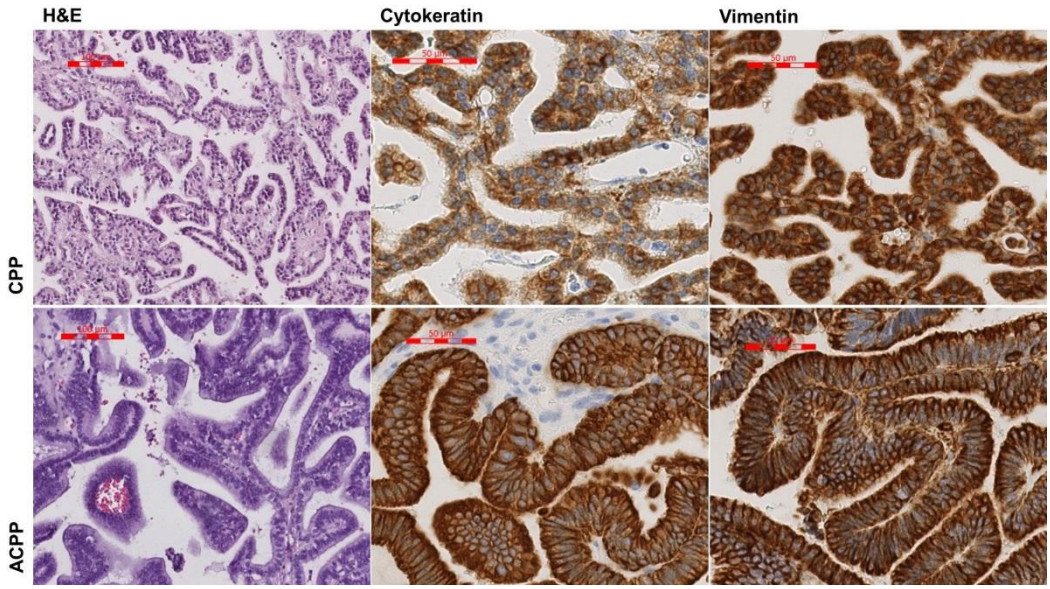

Figure 14C: CPP and ACPP H&E preparation and immunohistochemical analysis for vimentin and cytokeratin.

To exclude any malfunction in the Ubiquitin proteasome System (UPS) in the CCHE45 cell line proteasome activity was tested. UPS failure may result in accumulation of misfolded proteins in the form of aggresomes. CCHE-45 was compared with two other cell lines SHSY-5Y and SKNAS cell lines, (Figure 15) using proteosome assay loading solution (Abcam), and measured at EX/EM 490/620.

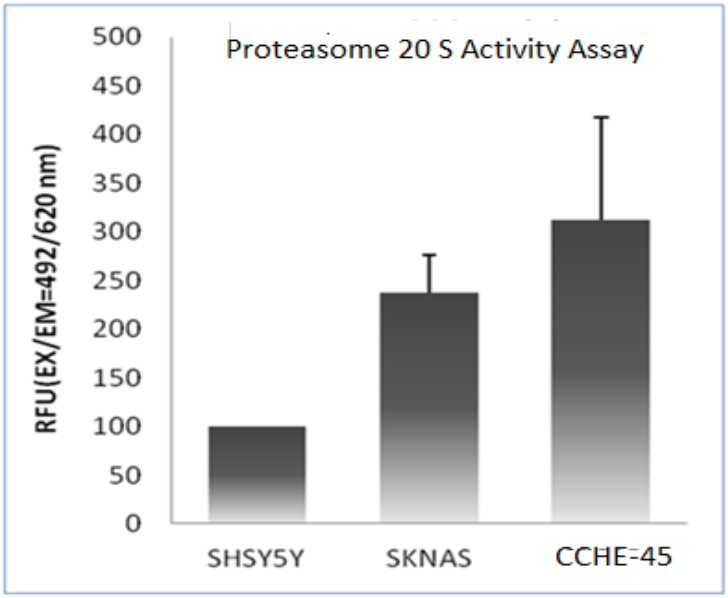

Figure 15: Proteasome activity assay comparing CCHE45 with SHSY5Y and SKNAS cell lines 20S activity was measured according to protocol, relative fluorescence intensity was measured with a plate reader.CCHE45 showed high activity.

Misfolded or aggregated proteins that cannot be eliminated by the proteosome are concentrated by HDAC6 and transported by the action of the dynein motor protein to the aggresomes. It has been previously shown that inhibitors of HDAC6 have an antitumor effect when coupled with conventional therapy. In this context, we evaluated the effect of different concentration of tubacin and its inactive analog niltubacin on CCHE-45 cells. Significant reduction in CCHE-45 proliferation was reported in a dose-dependent manner with no change in niltubacin treated cells (p-value = 0.01) (Figure 16).

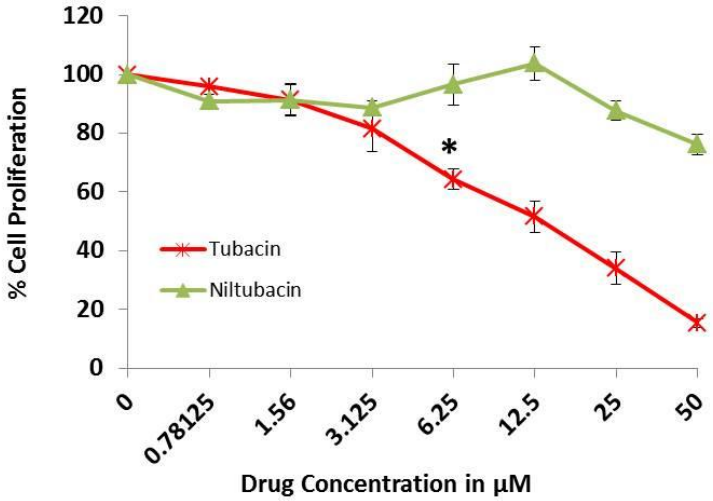

Figure 16: The effect of tubacin and niltubacin on CCHE-45 cell line was evaluated by cell viability assay. Cells were treated with different concentration of both drugs for 48 hours before treating with WST-1 for 4 hours; absorbance was then read at 440 nm. Results were averaged over three separate experiments. Error bars represent ± S.E.M, represent significant p-value where $p \leq 0.05$.

Treatment with tubacin resulted in the increase of acetylated α-tubluin and no change in vimentin protein levels (Figure 17), supporting the known effect of tubacin as an HDAC6 inhibitor on α-tubulin acetylation.

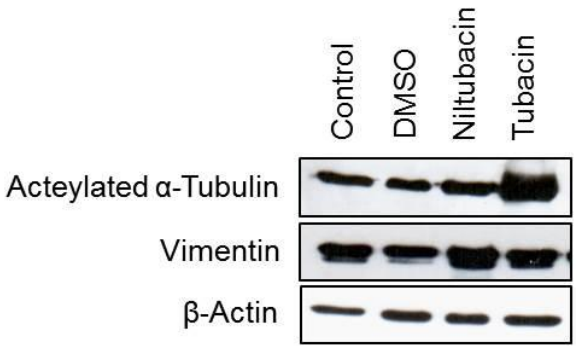

Figure 17: Immunoblot analysis for CCHE-45 after treatment with DMSO, tubacin (15µM), niltubacin (15µM) or non-treated (control). β-actin was used as a loading control.

Furthermore, due to the significant effect of tubacin on CCHE-45 proliferation, we hypothesized that tubacin treatment will result in disappearance of aggresomes as a consequence to HDAC6 inhibition. Despite HDAC6 inhibition, aggresomes were detected in tubacin treated cells however, they presented mainly as hollow cage structures (Figure 18).

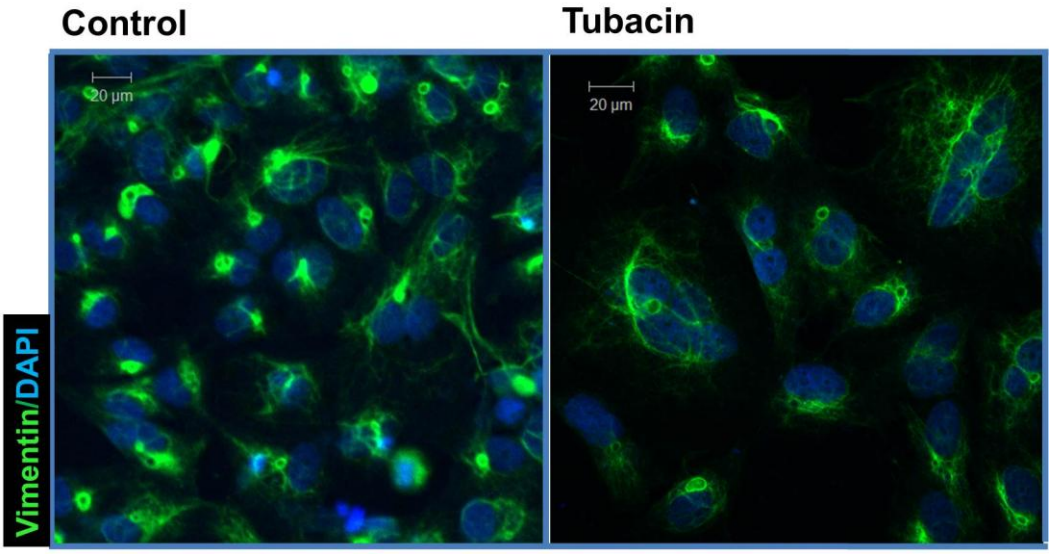

Figure 18: Immunofluorescence staining of CCHE-45 cells treated with 15µM of tubacin for 48 hours. CCHE-45 cells were immunostained with vimentin (green) and counterstained using DAPI.

3-2:Effect of nutrient deprivation on autophagy markers and aggresome clearence .

The presence of aggresomes has been linked to cellular proteotoxic overload that cannot be eliminated by the proteasome. Consequently autophagy becomes the main route for aggresomes clearance. To further address the contribution of autophagy to the observed phenotype, we treated CCHE-45 cells with HBSS for 2 and 6 hours. The induction of autophagy was initially monitored by the change in LC3B and LC3A processing. While LC3B and LC3A protein levels were reduced in the neuroblastoma line SH-SY5Y after nutrient deprivation for 2 and 6 hours (Figure 19), CCHE-45 cells displayed reduction in LC3B with no detectable LC3A protein in control cells and no change in vimentin levels (Figure 19).

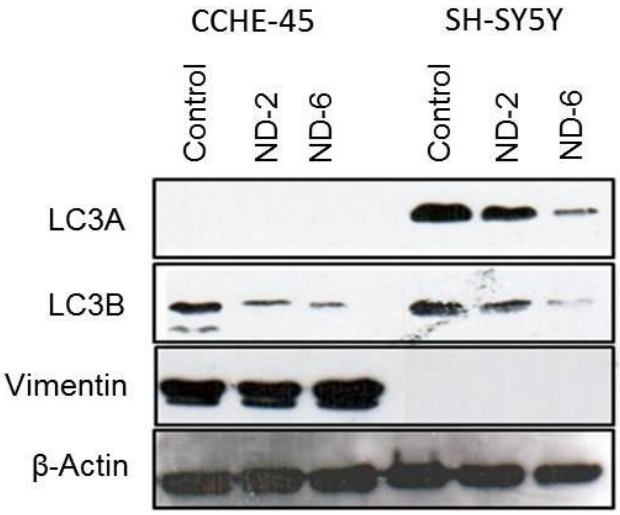

Figure 19: CCHE-45 and SH-SY5Y cells were cultured under normal condition or serum starved for 2 or 6 hours in HBSS. Whole cell lysates were collected and analyzed by Western blot analysis. β-actin was used as a loading control.

Due to potential cross-reactivity between available antibodies for both LC3A and LC3B, both proteins immunoblots were always performed on separate membranes. The reduction in LC3B levels and the lack of change in vimentin protein levels following nutrient deprivation suggested no effect on aggresome clearance, accordingly IF was further used to monitor autophagy in both cell lines. IF for LC3B primarily showed nuclear localization under control condition and formed cytoplasmic puncta upon nutrient deprivation in CCHE-45 (Figures 20A) confirming autophagy. Furthermore, both LC3B and the lysosomal marker LAMP2 co-localized with each other or with vimentin upon induction of autophagy (Figure 20A).

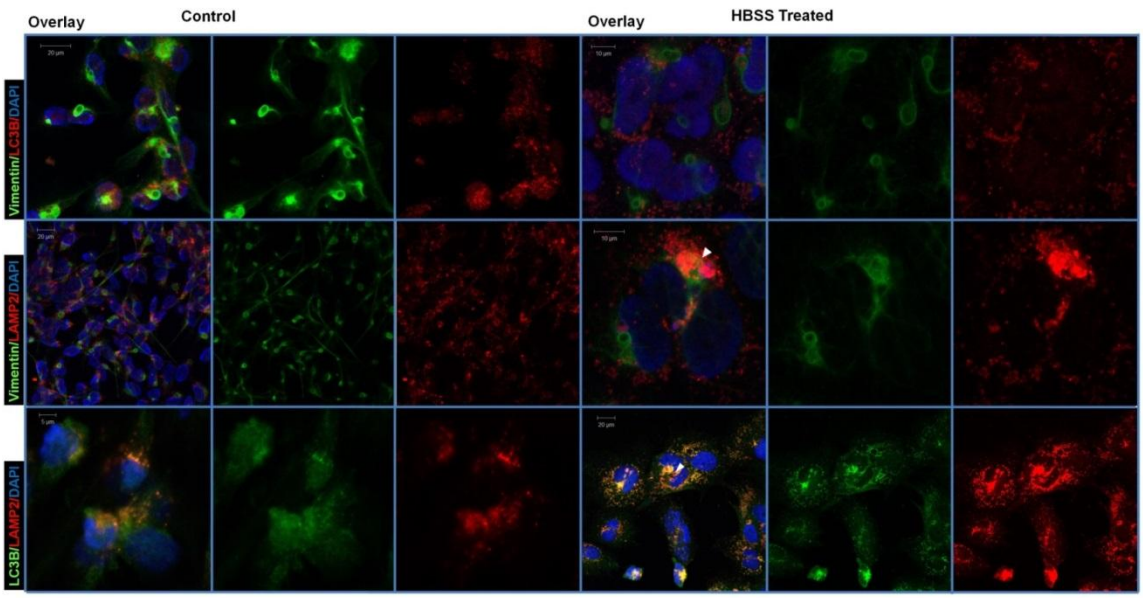

Figure 20A: Cells were cultured under normal condition or serum starved in HBSS for 2 hours. CCHE-45 cells were coimmunostained with vimentin and LC3B, vimentin and LAMP2 or LC3B and LAMP2. Cells were fixed in 4% paraformaldehyde, immunostained with anti-LC3B, anti-LC3A, anti-vimentin or anti-LAMP2 and visualized using Alexa Fluor 488 goat anti-rabbit antibody or Alexa Fluor 555 goat anti-mouse.

However, upon autophagy induction LC3A co-localized with LC3B either to the aggresomes or to other cellular sites (Figure 20A). LC3B was primarily nuclear in SH-SY5Y under normal conditions while LC3A protein was detected in the cytoplasm and the nucleus (Figure 20B). When treated with HBSS for 2 hours, LC3B displayed a cytoplasmic puncta indicative of autophagy induction while LC3A became entirely cytoplasmic with some co-localization with LC3B protein. On the other hand LAMP2 co-localized with both LC3A and LC3B (Figure 20B).

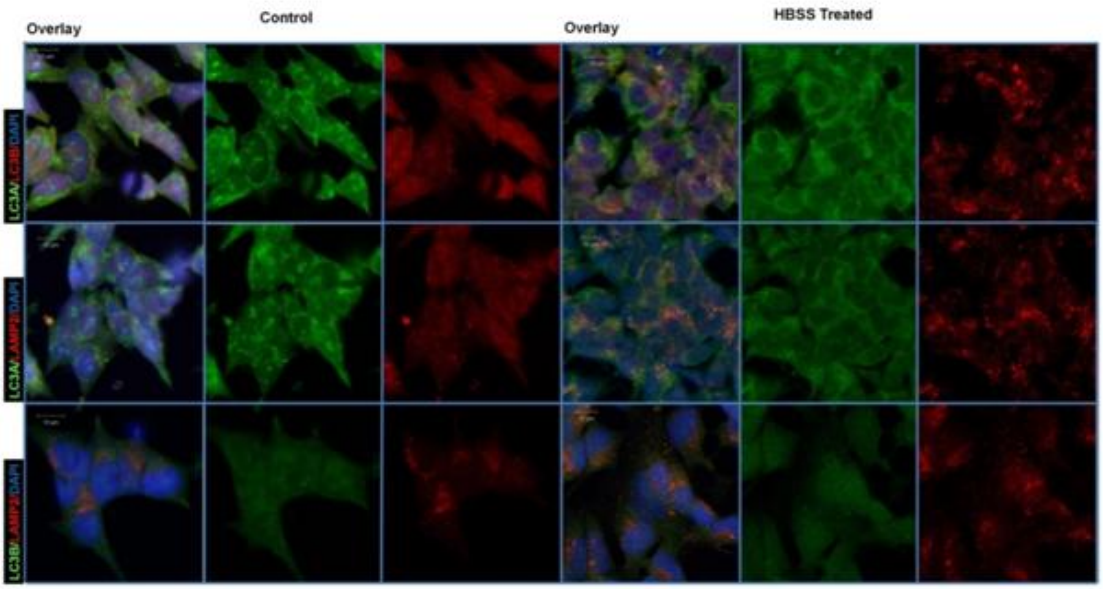

Figure 20B: SH-SY5Y cells were cultured under normal condition or serum starved in HBSS for 2 hours. Cells were fixed in 4% paraformaldehyde, immunostained with anti-LC3B, anti-LC3A, anti- LC3A and LAMP2 or LC3B and LAMP2. Cells were visualized using Alexa Fluor 488 goat anti-rabbit antibody or Alexa Fluor 555 goat anti-mouse. DAPI was used as counterstain to visualize the nucleus.

Despite the induction of autophagy, aggresomes were detected in CCHE-45 cells, however they formed hollow ring like structures similar to tubacin treated cells suggestive of altered vimentin assembly. TEM for CCHE-45 cells showed autophagic vacuoles present in close proximity to aggresomes

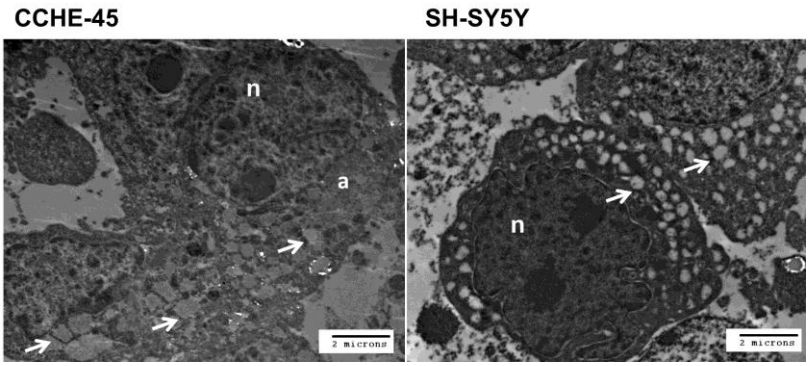

Figure 20 C: TEM examination CCHE-45 and SH-SY5Y cells using JEOL (JEM-1400 T). Cells were serum starved in HBSS for 2 hours before fixation for TEM analysis**.** a = aggresomes, n = nucleus, white arrow = autophagic vacuoles

3-3: Silencing of *LC3A-V1* expression in choroid plexus carcinoma tumors by intergenic CpG island methylation

Recent reports have shown that LC3A expression is absent in several tumors and corresponds to poor prognosis. The absence of LC3A protein in CCHE-45 coupled with previous reports of epigenetic inactivation of *LC3A-V1* in a number of tumors incited us to test for its silencing in CCHE-45 cells . To verify that the lack of expression of LC3A in CCHE-45 is not related to the tissue of origin, BrainSpan transcriptome dataset were used to examine the expression of LC3A and LC3B in normal brain tissues (Figure 21).

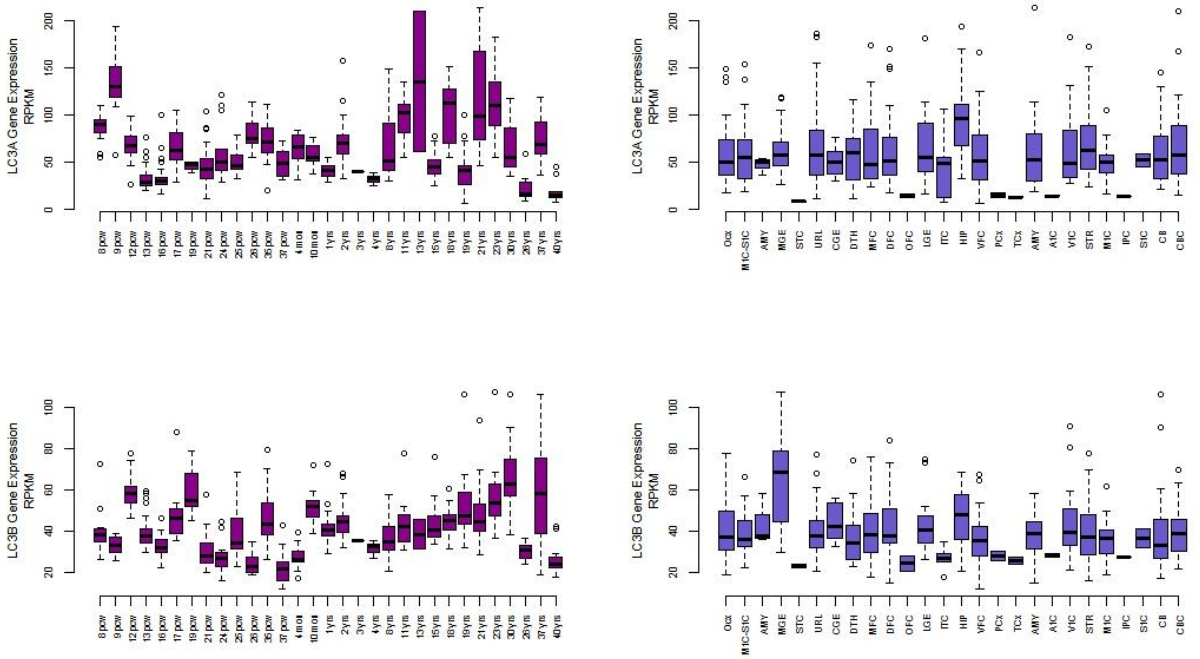

Figure 21: LC3A and LC3B gene expression as a function of different developmental stages (upper panel) and as a function of different regions in the brain (lower panel) using RNA-Seq data from the BrainSpan Project. Expression of LC3A and LC3B were detected in all developmental stages and at different part of the brain. pcw = post conception weeks, mon = month, yrs = years, Ocx = occipital neocortex, M1C-S1C = primary motor-sensory cortex, AMY = amygdaloid complex, MGE = medial ganglionic somatosensory

LC3A and LC3B were found to be expressed in all brain regions and during different developmental stages. *LC3A* gene has been recently shown to have two transcriptional variants which differ in transcription start site (Figure 22).

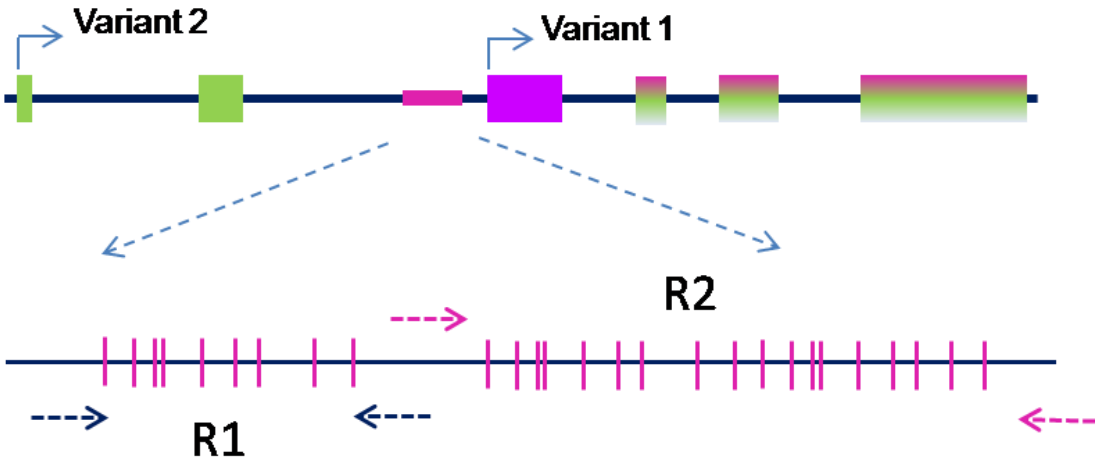

Figure 22: Schematic representation of *LC3A* exon-intron structure showing the difference in transcriptional start site between *LC3A-V1* and *LC3AV-2* (Bai et al, 2012).

Expression of both *LC3A* variants were absent in CCHE-45 cells, while only *LC3A-V1* was present in SH-SY5Y cells, supporting that variant one is the predominant variant (Figure 23).

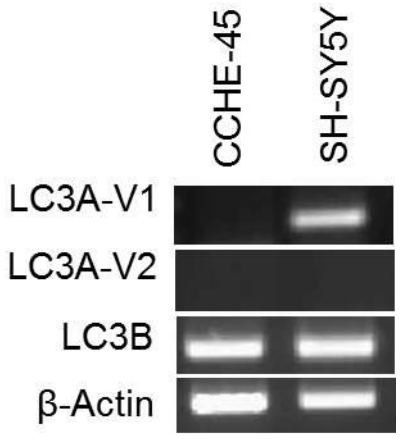

Figure 23: Expression of *LC3A –V1*, V2 and *LC3B* were examined using RT-PCR in CCHE-45 and SH-SY5Y cells. β-actin was used as an internal control.

Furthermore, examining both LC3A and LC3B in the parent tumor tissue supports that inactivation of the former (Figure 24).

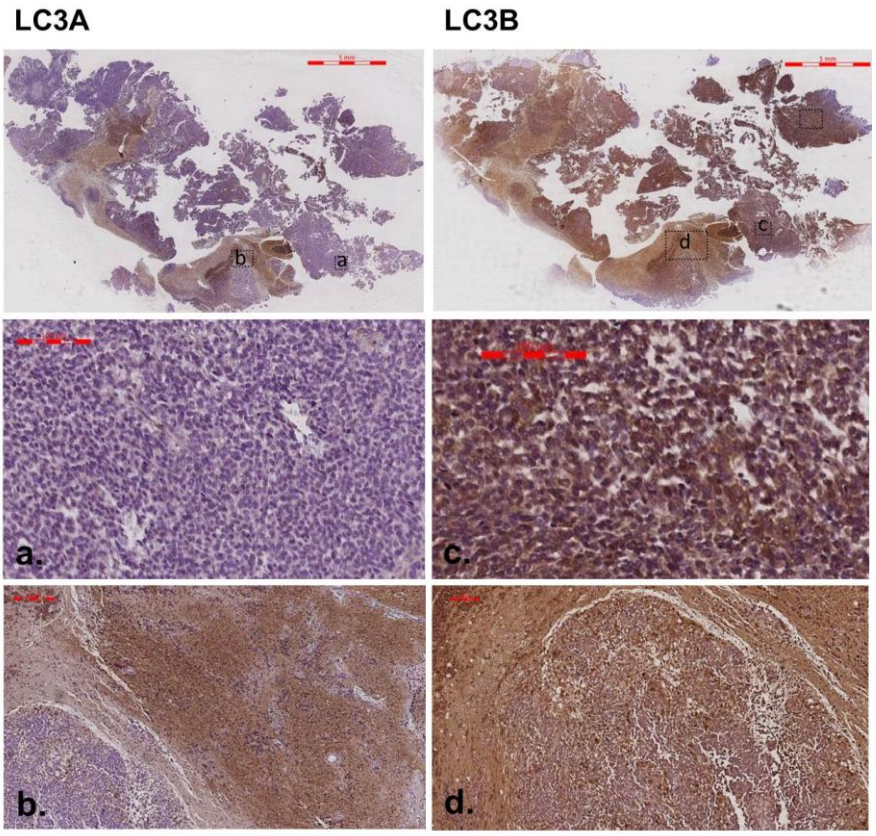

Figure 24: Immunohistochemical analysis for LC3A and LC3B expression in CCHE-45 original tumor. LC3A was detected in normal brain tissue (region a) while tumor area (region b) was negative for LC3A expression. On the other hand LC3B expression was detected in normal and tumor tissue region (c and d) respectively.

We further examined the CpG island status of *LC3A-V1* CCHE-45 in comparison to SH-SY5Y which is previously reported to be methylated in a wide range of tumors including multiple myeloma cells which are known to form aggresomes. Concordant with this data, is the fact that

Loss of *LC3A-V1* expression in CCHE-45 was due to intergenic CpG island methylation (Figure 25A). Bisulfite sequencing of CCHE-45 parent tumor indicated complete promoter methylation in all ten clones examined (Figure 25B).

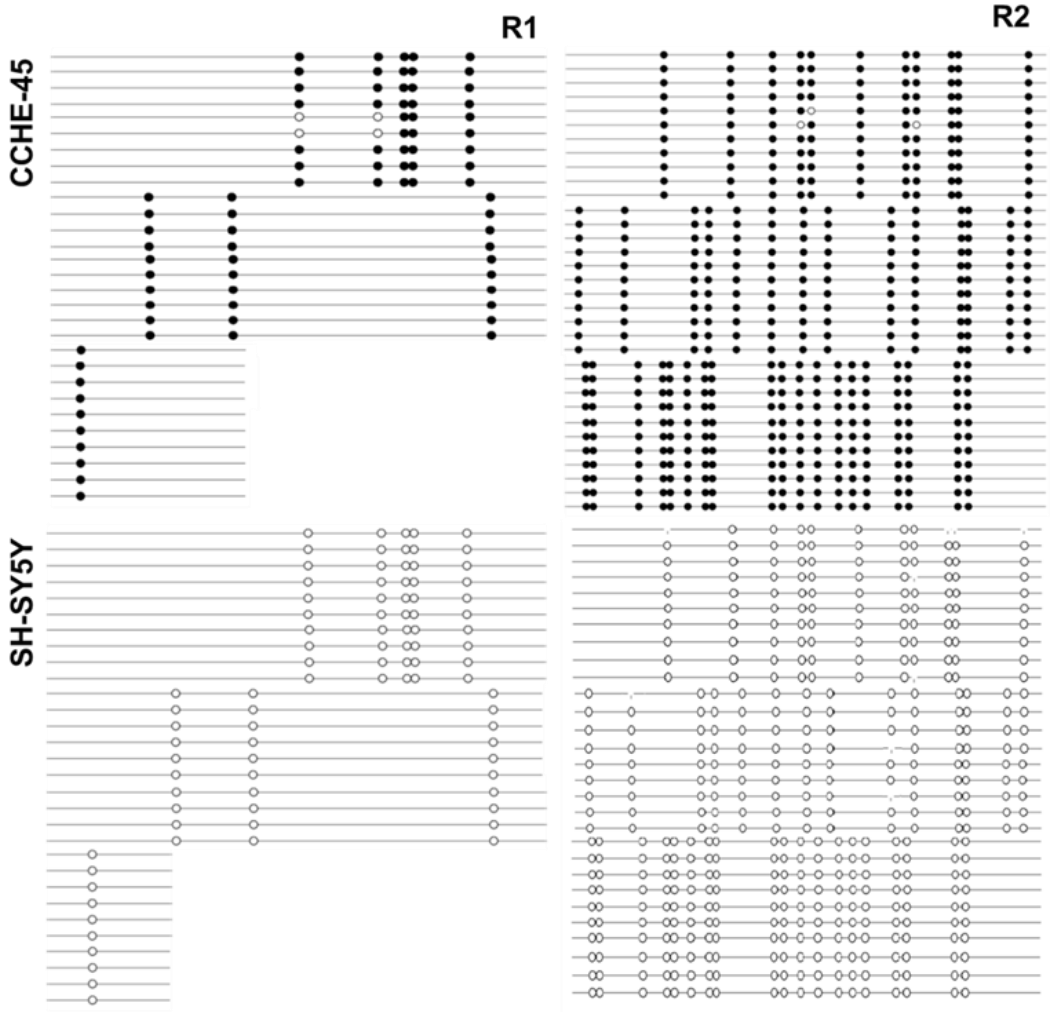

Figure 25A: Bisulfite modified DNA PCR products from CCHE-45 and SH-SY5Y, the diagrams show methylated CG dinucleotide in CCHE-45 R1 and R2 (closed circles) with no methylation detected in SH-SY5Y (open circles). Primers were designed to amplify region 1 and region 2 (R1 and R2 respectively) to examine the methylation status of CpG island upstream of *LC3A-V1* using bisulfite sequencing.

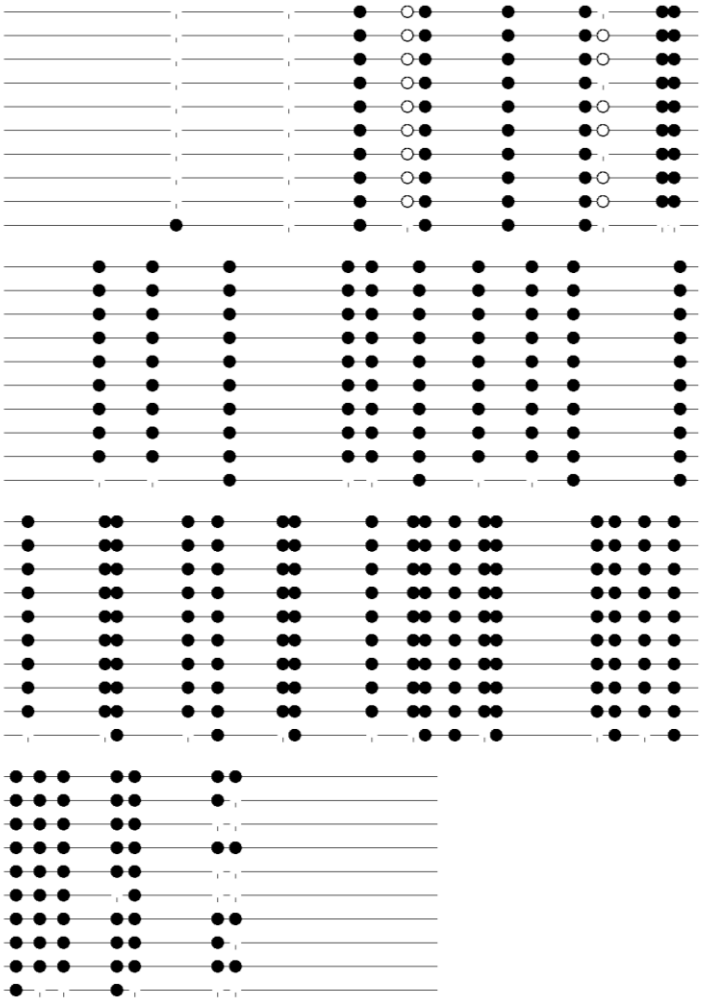

Figure 25B: Bisulfite sequencing for CCHE-45 original tumor. Region 2 was amplified using R2 primer set. Methylated CG dinucleotide is indicated by closed circles.

Further treatment of CCHE-45 with the general demethylating agent 5-Aza-2-deoxycytidine (5-AZA-dC) resulted in the re-expression of *LC3A* (Figure 26), supporting the role of methylation in the regulation of *LC3A-V1* expression.

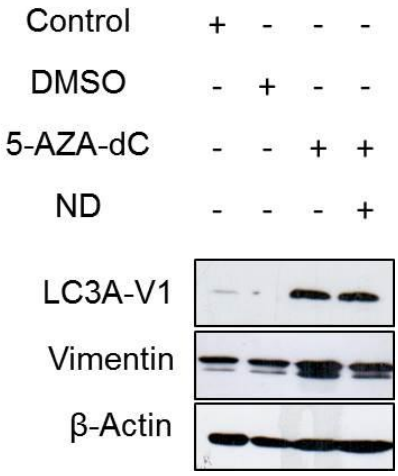

Figure 26: Western blot analysis for CCHE-45 cells treated with 10µm 5-AZA-dC for 4 days then serum starved in HBSS for 2 hrs. LC3A protein was restored following 5-AZA-dC treatment. No change in vimentin expression was detected.

We next examined the expression of both genes in CPTs using immunohistochemical analysis. While LC3B expression was detected in all tumors, LC3A expression was positive in CPP and either focal or absent in both ACPP and CPC (Figure 27).

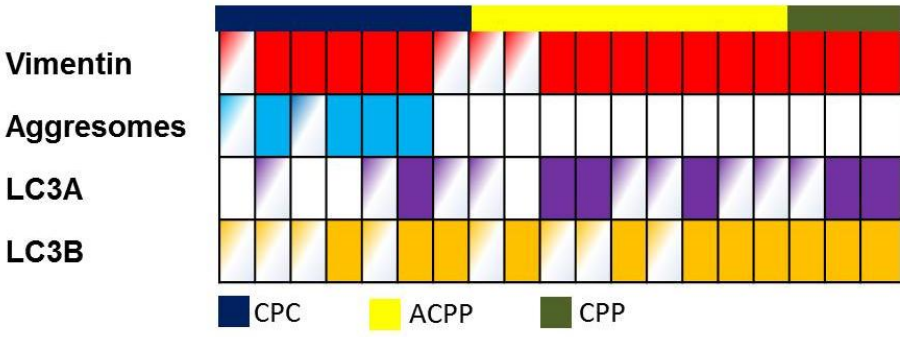

Figure 27: Schematic representation for immunostaining for 19 cases choroid plexus carcinoma (blue), atypical choroid plexus carcinoma (yellow) or choroid plexus papilloma (olive) stained with vimentin, LC3A or LC3B. Solid, partial and clear color indicates positive, focal and negative stain respectively.

3.4-LC3A re-expression induces aggresome clearance by lysosomal recruitment that is independent of autophagosome formation.

Because of the correlation between aggresomes and *LC3A*-V1 silencing, we reasoned that the lack of expression in CPC may affect aggresomes accumulation. To further elucidate the role of LC3A, we cloned *LC3A-V1* or *LC3A-V2* cDNA downstream of a CMV promoter and transiently transfected CCHE-45 cells with empty vector or *LC3A-V1* or *LC3A-V2*. Transfection efficiency was monitored by GFP positivity. The expression of LC3A was further confirmed by immunoblot analysis (Figure 28). A decrease in LC3B was observed in *LC3A-V1* transfected cells (Figure 28).

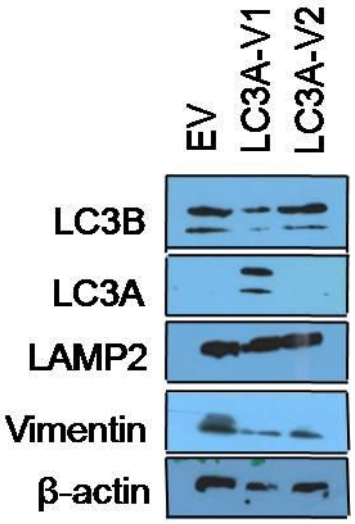

Figure 28: Western blot analysis for CCHE-45 transfected with p-IRES2-AcGFP empty vector (EV), p-IRES2-AcGFP-LC3A-V1 (LC3A-V1) or p-IRES2-AcGFP-LC3A-V2 (LC3A-V2).

To visualize the effect of LC3A on aggresomes, CCHE-45 cells were immune-stained for vimentin 48 hours post transfection. Consistent with 5AZA-dC treatment, LC3A displayed a cytoplasmic filament like appearance (Figure 29). Furthermore, less number of aggresomes was observed and vimentin displayed a filament like organization or hollow circles rather than dense localized peri-nuclear inclusions (Figure 29). Furthermore, LC3A mainly surrounded the aggresomes forming a ring around the inclusion or was in close proximity with minimal colocalization. LAMP2 co-localized with LC3A and surrounded the aggresomes as well as detected within the aggresomes (Figure 29).

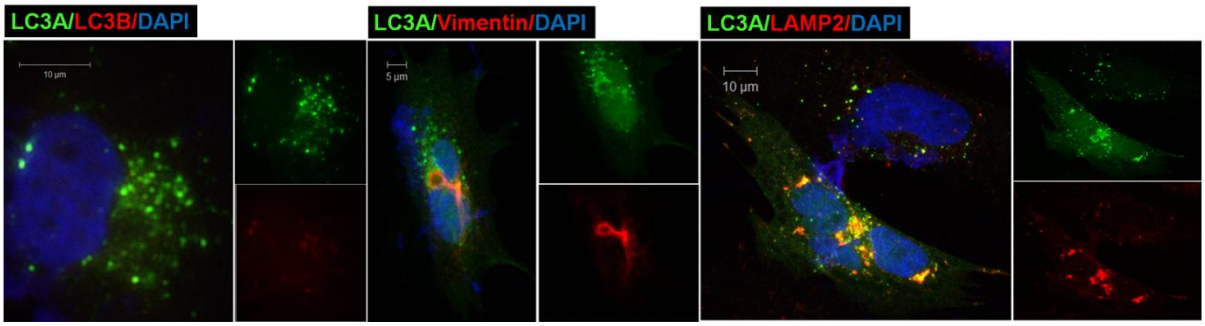

Figure 29: Immunofluorescence analysis of CCHE-45 cells transfected with p-IRES2-AcGFP empty vector) or p-IRES2-AcGFP-LC3A-V1. Cells were immunostained with LC3A and LC3B, vimentin and LC3A or LC3A and LAMP2 and visualized using Alexa Fluor 488 goat anti-rabbit antibody or Alexa Fluor 555 goat anti-mouse. The figure shows the disappearance of aggresomes and the colocalization with LAMP2 in p-IRES2-AcGFP-LC3A-V1 transfected cells.

4-DISCUSSION

Mutations, metabolic challenges and stress conditions are common reasons for the production of aberrant proteins (Chen, Retzlaff, Roos, & Frydman, et al., 2011). Consequently, cells exert several quality control strategies aimed at refolding (Hartl, Bracher, & Hayer-Hartl, 2011), degrading or sequestering aberrant protein species (Heck, Cheung, & Hampton, 2010). Insoluble protein deposit (IPOD) and intranuclear quality control (INQ) are two compartments for protein sorting and sequestration for cytoplasmic and nuclear proteins, respectively (Chen, Retzlaff, Roos, & Frydman, et al., 2011, Miller et al., 2005). Additionally, aggresomes are specialized, cytoplasmic cage-like structures that form at the microtubule organizing centers (MTOC) to sequester misfolded proteins (Kawaguchi, Kovacs, McLaurin, Vance, et al., 2003). The role of protein sequestration into inclusion bodies in cancer is not well defined. Here we report the development of a new choroid plexus carcinoma cell line CCHE-45. The cells were characterized by the presence of a single cage like inclusion body at juxtanuclear position that was positive for vimentin. These structures have been identified previously as aggresomes (Johnston et al., 1998). Recently, the JUxta Nuclear Quality control compartment (JUNQ) was used to describe vimentin positive structures that share similar cellular position as aggresomes (Kaganovich, Kopito, & Frydman, 2008).Furthermore, it was proposed that aggresomes may represent a mature state of JUNQ (Heck, Cheung, & Hampton, 2010). In the case of CCHE-45 cells, their constitutive presence in all cells and lack of mobility supports aggresome description rather than JUNQ. While most reports suggest that aggresomes are formed by single intermediate filaments (Johnston et al., 1998, Saliba, Munro, Luthert, & Cheetham, 2002), we find that both cytokeratin and vimentin contribute to the cage like structure of aggresomes in CPC. The absence of aggresomes in both CPP and ACCP and their presence in CPC supports the notion that their accumulation is more likely to be associated with aggressive tumors. The formation of aggresomes was shown to be dependent on the collection of aggregates by HDAC6 and dynin motor proteins (Kawaguchi, Kovacs, McLaurin, Vance, et al., 2003). The significant decrease in cell proliferation following treatment with tubacin highlights the role of aggresomes as a protective mechanism against aberrant proteins. Furthermore, the disassembly of aggresomes following HDAC6 inhibition with no change in vimentin protein levels suggests that aggresome assembly is coupled to aggregates transport (Kawaguchi, Kovacs, McLaurin, Vance, et al., 2003).

While aggresomes are considered a cytoprotective mechanism, they are ultimately eliminated by autophagy. Monitoring autophagy has proven to be challenging due to difference in tissue response to stress as well as limitations associated with different assays (Klionsky, 2016). LC3B is commonly used as a marker for induction of autophagy (Tanida, Ueno, & Kominami, et al., 2005); however MAP1LC3/LC3 family members encompass LC3A, LC3B and LC3C where the former two have been reported to participate in autophagosome formation (Shpilka, Weidberg, Pietrokovski, & Elazar, 2011, Koukourakis, Kalamida, Giatromanolaki, Zois, et al., 2015). Examining both LC3A and LC3B following nutrient deprivation, we find that both proteins are present and processed to form cytoplasmic puncta indicative of autophagy activation in SH-SY5Y cells. In contrast, LC3B presented with both bands (LC3B-I and LC3B-II) under normal growth condition and no detectable LC3A protein in CCHE-45 cells. The increased signal for autophagosome detected by the presence of lipdiated form of LC3B and the cytoplasmic puncta for LC3B supports the activation of autophagy at a basal level in CCHE-45 cells. At the same time, the decrease in LC3B-I and LC3B-II protein levels following nutrient deprivation supports the notion of enhanced autophagy flux in CCHE-45 cells. Based on these results we propose that CCHE-45 cells exhibit enhanced autophagy flux to overcome proteotoxic stress. Furthermore, the disassembly of the vimentin cage following autophagy induction supports the role of induced autophagy as a regulator of aggresomes. By inducing non-selective macroautophagy aberrant proteins are removed which in turn results in altered assembly of the vimentin cage rather than removal of aggresomes by engulfment. This notion is further supported by TEM for CCHE-45 cells showing autophagic vacuoles present in close proximity to aggresomes. This is in line with previous reports for autophagic vacuoles and lysosome recruitment to aggresomes to facilitate its degradation following proteasome inhibition (Zaarur, Meriin, Bejarano, Xu, et al., 2014).

Deregulation of signalling pathways and microtubule associated proteins which have been shown to correlate with the clinical outcomes in some tumors. For instance LC3B-II down regulation correlated with poor survival in GBM (Huang, Bai, Chen, Li, & Lu, 2010) and the loss of LC3A expression by promoter-silencing was found in different tumor cell lines (Bai, Inoue, Kawano, & Inazawa, 2012). Furthermore, both LC3A and LC3B were found to form stone like structures which correlated with poor prognosis (El-Mashed, O'Donovan, Kay, Abdallah, Cathcart, & O'Sullivan, et al.,2015). Analysis of BrainSpan RNA-Seq data identifies LC3A and LC3B to be ubiquitously expressed in the brain during different developmental stages. While LC3B is expressed in CCHE-45 cells, *LC3A-V1* was silenced by

promoter methylation in CCHE-45 and primary CPC supporting previous reports of *LC3A-V1* inactivation. Interestingly, multiple myeloma, which is known to form aggresomes, shows inactivation of LC3A-V1 by the same mechanism. These results support a potential correlation between *LC3A-V1* gene silencing and the development of aggresomes. The disassembly of the vimentin cage following LC3A-V1 expression coupled with recruitment of LAMP2 independent of LC3B suggestive of autophagy activation independent of macroautophagy. These results support the hypothesis that under the stress imposed by protein overload, LC3A modulates cellular basal quality control.

In conclusion, protein misfolding and aggregation has been mainly investigated in neurological disorders. In cancer, understanding cellular response to aberrant protein which is a common feature to cancer cells has been primarily investigated using ectopic expression of aberrant proteins coupled with proteasome inhibitors. CCHE-45 cells provide a new model for understanding aggresome dynamics without disruption of tumor environment. Moreover, it serves as a new model to investigate how cancer cells employ autophagy quality-control to achieve proteostasis highlighting a new role for LC3A protein. Finally our work identifies aggresomes as a potential new molecular target for CPC and other tumors with a similar phenotype.

5-FUTURE DIRECTION

In our research we were mainly investigating the vimentin cage forming the aggresomal structure; our next step is to study the expression of the intermediate filament cytokeratin. Cytokeratin was found to contribute to the structure of aggresomes formation in our cell line and the original tumor. As with the vimentin expression we will study the effect of HDAC6 inhibitor on cell proliferation. Autophagy activation by nutrient deprivation and how would it affect the cytokeratin structure and concentration would be further studied. We will also study the effect of treatment with a demethylating agent such as 5-Aza-dC and transfection with LC3A gene on the structure of the cytokeratin and compare it with the effect on the vimentin cage. In addition, we need to further study the different component contributing in the aggresome structure other than vimentin and cytokeratin.

In this thesis study we were mainly concerned about the mechanisms contributing to clearance of the aggresomes such as the ubiquitin proteasomal pathway and autophagy. Our next aim is to tackle the mechanisms that lead to its formation in the first place. The different stresses that lead to protein misfolding and the reason they ended up contained by aggresomes from their ubiquitination status to solubility will be further investigated.

A recent study showed an asymmetric segregation of aggresomes during mitosis, we plan to study the fate of aggresomes during cell division in CCHE-45, using different molecular biology techniques and many cytological assays. We will investigate whether the cell line will undergo normal mitosis. The segregation pattern of the aggresomes whether symmetric or asymmetric will be compared with other cell lines.

At last we would like to target the aggresomes with different potent and selective new generation inhibitors such as Tubastatin A, we will verify its effect on cell proliferation, vimentin and cytokeratin expression and aggresomal clearance. Ultimately, we hope to able to find a potential target in choroid plexus carcinoma that can be used for future treatment.

6-REFERENCES

Abraham, R. T. (2001). Cell cycle checkpoint signaling through the ATM and ATR kinases. *Genes Dev, 15*(17), 2177-2196.

Bai, H., Inoue, J., Kawano, T., & Inazawa, J. (2012). A transcriptional variant of the LC3A gene is involved in autophagy and frequently inactivated in human cancers. *Oncogene, 31*(40), 4397-4408.

Bruijn, L. I., Houseweart, M. K., Kato, S., Anderson, K. L., Anderson, S. D., Ohama, E., et al. (1998). Aggregation and motor neuron toxicity of an ALS-linked SOD1 mutant independent from wild-type SOD1. *Science, 281*(5384), 1851-1854.

Bunz, F. (2008). Principals of cancer of Genetics. *Baltimore,Springer science*.pp 5-47

Camaco, J. (2012). Molecular oncology:principles and recent advances. *Mexico:Bentham science publisher*.pp 219-222.

Chen, B., Retzlaff, M., Roos, T., & Frydman J. (2011). Cellular Strategies of Protein Quality Control. *Cold Spring Harb Perspect Biol, 3*(8), 4374.

Chen, Y., & Klionsky, D. J. (2011). The regulation of autophagy - unanswered questions. *J Cell Sci, 124*(Pt 2), 161-170.

Chi, P., Allis, C. D., & Wang, G. G. (2010). Covalent histone modifications--miswritten, misinterpreted and mis-erased in human cancers. *Nat Rev Cancer, 10*(7), 457-469.

Croce, C. M. (2008). Oncogenes and cancer. *N Engl J Med, 358*(5), 502-511.

Dienstmann, R., Rodon, J., Serra, V., & Tabernero, J.(2014) Picking the point of inhibition: a comparative review of PI3K/AKT/mTOR pathway inhibitors. *Mol Cancer Cel, 13*(5):1021-1031.

DiFiglia, M., Sapp, E., Chase, K. O., Davies, S. W., Bates, G. P., Vonsattel, J. P., et al. (1997). Aggregation of huntingtin in neuronal intranuclear inclusions and dystrophic neurites in brain. *Science, 277*(5334), 1990-1993.

Driscoll, J. J., & Chowdhury, R. D. (2012). Molecular crosstalk between the proteasome, aggresomes and autophagy: translational potential and clinical implications. *Cancer Lett, 325*(2), 147-154.

Efeyan, A., & Sabatini, D. M.(2010). mTOR and cancer: many loops in one pathway. *Curr Opin Cell Biol, 22*(2), 169-176.

El-Gaidi, M. A. (2011). Descriptive epidemiology of pediatric intracranial neoplasms in Egypt. *Pediatr Neurosurg, 47*(6), 385-395.

El-Mashed, S., O'Donovan, T.R., Kay, E.W., Abdallah, A.R., Cathcart, M.C., & O'Sullivan, J., et al. (2015). LC3B globular structures correlate with survival in esophageal adenocarcinoma. *BMC Cancer. 15*, 580-582.

Engelman, J. A., Luo, J., & Cantley, L. C. (2006). The evolution of phosphatidylinositol 3-kinases as regulators of growth and metabolism. *Nat Rev Genet, 7*(8), 606-619.

Finnin, M. S., Donigian, J. R., Cohen, A., Richon, V. M., Rifkind, R. A., Marks, P. A., et al. (1999). Structures of a histone deacetylase homologue bound to the TSA and SAHA inhibitors. *Nature, 401*(6749), 188-193.

Fischer, A., Sananbenesi, F., Mungenast, A., & Tsai, L. H. (2010). Targeting the correct HDAC(s) to treat cognitive disorders. *Trends Pharmacol Sci, 31*(12), 605-617.

Fleming, A. J., & Chi, S. N. (2012). Brain tumors in children. *Curr Probl Pediatr Adolesc Health Care, 42*(4), 80-103.

Frech, M., Andjelkovic, M., Ingley, E., Reddy, K. K., Falck, J. R., & Hemmings, B. A. (1997). High affinity binding of inositol phosphates and phosphoinositides to the pleckstrin homology domain of RAC/protein kinase B and their influence on kinase activity. *J Biol Chem, 272*(13), 8474-8481.

Friedman, R. C., Farh, K. K., Burge, C. B., & Bartel, D. P. (2009). Most mammalian mRNAs are conserved targets of microRNAs. *Genome Res, 19*(1), 92-105.

Gao, X., Zhang, Y., Arrazola, P., Hino, O., Kobayashi, T., Yeung, R. S., et al. (2002). Tsc tumour suppressor proteins antagonize amino-acid-TOR signalling. *Nat Cell Biol, 4*(9), 699-704.

Garcia-Mata, R., Bebok, Z., Sorscher, E. J., & Sztul, E. S. (1999). Characterization and dynamics of aggresome formation by a cytosolic GFP-chimera. *J Cell Biol, 146*(6), 1239-1254.

Garcia-Mata, R., Gao, Y. S., & Sztul, E. (2002). Hassles with taking out the garbage: aggravating aggresomes. *Traffic, 3*(6), 388-396.

Glenner, G. G., & Wong, C. W. (1984). Alzheimer's disease: initial report of the purification and characterization of a novel cerebrovascular amyloid protein. *Biochem Biophys Res Commun, 425*(3), 534-539.

Gopal, P., Parker, J. R., Debski, R., & Parker, J. C., Jr. (2008). Choroid plexus carcinoma. *Arch Pathol Lab Med, 132*(8), 1350-1354.

Grasso, D., Ropolo, A., & Vaccaro, M. (2015). Autophagy in Cell Fate and Diseases, Cell Death - Autophagy, Apoptosis and Necrosis.

Groll, M., & Huber, R. (2003). Substrate access and processing by the 20S proteasome core particle. *Int J Biochem Cell Biol, 35*(5), 606-616.

Hanahan, D., & Weinberg, R. A. (2011). Hallmarks of cancer: the next generation. *Cell, 144*(5), 646-674.

Hartl, F.U., Bracher, A., & Hayer-Hartl, M. (2011). Molecular chaperones in protein folding and proteostasis. *Nature*. *475*(5), 324–332.

Hasselblatt, M., Bohm, C., Tatenhorst, L., Dinh, V., Newrzella, D., Keyvani, K., et al. (2006). Identification of novel diagnostic markers for choroid plexus tumors: a microarray-based approach. *Am J Surg Pathol, 30*(1), 66-74.

Hasselblatt, M., Muhlisch, J., Wrede, B., Kallinger, B., Jeibmann, A., Peters, O., et al. (2009). Aberrant MGMT (O6-methylguanine-DNA methyltransferase) promoter methylation in choroid plexus tumors. *J Neurooncol, 91*(2), 151-155.

Heck J.W., Cheung S.K., & Hampton R.Y. (2010).Cytoplasmic protein quality control degradation mediated by parallel actions of the E3 ubiquitin ligases Ubr1 and San. *Proc Natl Acad Sci.107*, 1106–1111.

Henikoff, S., & Ahmad, K. (2005). Assembly of variant histones into chromatin. *Annu Rev Cell Dev Biol, 21*, 133-153.

Hennessy, B. T., Smith, D. L., Ram, P. T., Lu, Y., & Mills, G. B. (2005). Exploiting the PI3K/AKT pathway for cancer drug discovery. *Nat Rev Drug Discov, 4*(12), 988-1004.

Hershko, A., & Ciechanover, A. (1998). The ubiquitin system. *Annu Rev Biochem, 67*, 425-479.

Ho, A. S., Turcan, S., & Chan, T. A. (2013). Epigenetic therapy: use of agents targeting deacetylation and methylation in cancer management. *Onco Targets Ther, 6*, 223-232.

How Kit, A., Nielsen, H. M., & Tost, J. (2012). DNA methylation based biomarkers: practical considerations and applications. *Biochimie, 94*(11), 2314-2337.

Huang, X., Bai, H. M., Chen, L., Li, B., & Lu, Y. C. (2010). Reduced expression of LC3B-II and Beclin 1 in glioblastoma multiforme indicates a down-regulated autophagic capacity that relates to the progression of astrocytic tumors. *J Clin Neurosci*, *17*, 1515–1519.

http://www.cbtrus.org/ (2013).

http:// www.hopkinsmedecine.org/

http:// https://www.iarc.fr/

Johansen, T., & Lamark, T. (2011). Selective autophagy mediated by autophagic adapter proteins. *Autophagy, 7*(3), 279-296.

Johnston, J., A., Ward, C., L.,& Kopito R., R. (1998). Aggresomes: A Cellular Response to Misfolded Proteins. *J Cell Biol*, *143*, 1883–1898.

Kabeya, Y., Mizushima, N., Ueno, T., Yamamoto, A., Kirisako, T., Noda, T., et al. (2000). LC3, a mammalian homologue of yeast Apg8p, is localized in autophagosome membranes after processing. *EMBO J, 19*(21), 5720-5728.

Kaganovich, D., Kopito, R., & Frydman, J. (2008). Misfolded proteins partition between two distinct quality control compartments. *Nature, 454*(7208), 1088-1095.

Kamaly-Asl, I. D., Shams, N., & Taylor, M. D. (2006). Genetics of choroid plexus tumors. *Neurosurg Focus, 20*(1), 10.

Kamihara, J., Rana, H. Q., & Garber, J. E. (2013). Germline TP53 Mutations and the Changing Landscape of Li-Fraumeni Syndrome. *Hum Mutat, 35*(6), 654-662.

Kamihara, J., Rana, H. Q., & Garber, J. E. (2014). Germline TP53 Mutations and the Changing Landscape of Li-Fraumeni Syndrome. *Hum Mutat, 35*(6), 654-662.

Kanwal, R., & Gupta, S. (2012). Epigenetic modifications in cancer. *Clin Genet, 81*(4), 303-311.

Kawaguchi, Y., Kovacs, J., J., McLaurin, A., Vance, J., M., et al. (2003). The Deacetylase HDAC6 Regulates Aggresome Formation and Cell Viability in Response to Misfolded Protein Stress. *Cell, 115*, 727–738.

Kim, D. H., & Sabatini, D. M. (2004). Raptor and mTOR: subunits of a nutrient-sensitive complex. *Curr Top Microbiol Immunol, 279*, 259-270.

Kirkin, V., Lamark, T., Johansen, T., & Dikic, I. (2009). NBR1 cooperates with p62 in selective autophagy of ubiquitinated targets. *Autophagy, 5*(5), 732-733.

Klionsky, D. J., Abeliovich, H., Agostinis, P., Agrawal, D. K., Aliev, G., Askew, D. S., et al. (2008). Guidelines for the use and interpretation of assays for monitoring autophagy in higher eukaryotes. *Autophagy, 4*(2), 151-175.

Koos, B., Paulsson, J., Jarvius, M., Sanchez, B. C., Wrede, B., Mertsch, S., et al. (2009). Platelet-derived growth factor receptor expression and activation in choroid plexus tumors. *Am J Pathol, 175*(4), 1631-1637.

Kopito, R. R. (2000). Aggresomes, inclusion bodies and protein aggregation. *Trends Cell Biol, 10*(12), 524-530.

Kosik, K. S., Joachim, C. L., & Selkoe, D. J. (1986). Microtubule-associated protein tau (tau) is a major antigenic component of paired helical filaments in Alzheimer disease. *Proc Natl Acad Sci U S A, 83*(11), 4044-4048.

Kravtsova-Ivantsiv, Y., & Ciechanover, A. (2012). Non-canonical ubiquitin-based signals for proteasomal degradation. *J Cell Sci, 125*(Pt 3), 539-548.

Lane, D. P., & Crawford, L. V. (1979). T antigen is bound to a host protein in SV40-transformed cells. *Nature, 278*(5701), 261-263.

Laplante, M., & Sabatini, D. M. (2009). mTOR signaling at a glance. *J Cell Sci, 122*(Pt 20), 3589-3594.

Lee, H. J., Shin, S. Y., Choi, C., Lee, Y. H., & Lee, S. J. (2002). Formation and removal of alpha-synuclein aggregates in cells exposed to mitochondrial inhibitors. *J Biol Chem, 277*(7), 5411-5417.

Lengauer, C., Kinzler, K. W., & Vogelstein, B. (1998). Genetic instabilities in human cancers. *Nature, 396*(6712), 643-649.

Levine, B., & Kroemer, G. (2008). Autophagy in the pathogenesis of disease. *Cell, 132*(1), 27-42.

Li, M., He, Y., Dubois, W., Wu, X., Shi, J., & Huang, J. (2012). Distinct regulatory mechanisms and functions for p53-activated and p53-repressed DNA damage response genes in embryonic stem cells. *Mol Cell, 46*(1), 30-42.

Lilienbaum, A. (2013). Relationship between the proteasomal system and autophagy. *Int J Biochem Mol Biol, 4*(1), 1-26.

Linzer, D. I., Maltzman, W., & Levine, A. J. (1979). The SV40 A gene product is required for the production of a 54,000 MW cellular tumor antigen. *Virology, 98*(2), 308-318.

Liu, Q., Thoreen, C., Wang, J., Sabatini, D., & Gray, N. S. (2009). mTOR Mediated Anti-Cancer Drug Discovery. *Drug Discov Today Ther Strateg, 6*(2), 47-55.

Loos, B., Engelbrecht, A. M., Lockshin, R. A., Klionsky, D. J., & Zakeri, Z. (2013). The variability of autophagy and cell death susceptibility: Unanswered questions. *Autophagy, 9*(9), 1270-1285.

Louis, D. N., Ohgaki, H., Wiestler, O. D., Cavenee, W. K., Burger, P. C., Jouvet, A., et al. (2007). The 2007 WHO classification of tumours of the central nervous system. *Acta Neuropathol, 114*(2), 97-109.

Lu, J., Getz, G., Miska, E. A., Alvarez-Saavedra, E., Lamb, J., Peck, D., et al. (2005). MicroRNA expression profiles classify human cancers. *Nature, 435*(7043), 834-838.

Miller, S., Ho, C.T., Winkler, J., Khokhrina, M., Neuner, A., et al. (2015) Compartment-specific aggregases direct distinct nuclear and cytoplasmic aggregate deposition. *EMBO J, 34*, 778–797.

Mizushima, N., Yoshimori, T., & Ohsumi, Y. (2011). The role of Atg proteins in autophagosome formation. *Annu Rev Cell Dev Biol, 27*, 107-132.

Morales, H., & Gaskill-Shipley, M. (2010). Imaging of common adult and pediatric primary brain tumors. *Semin Roentgenol, 45*(2), 92-106.

Muleris, M., Salmon, R., Zafrani, B., Girodet, J., & Dutrillaux, B. (1985). Rearrangement of the chromosome 17 in colonic adenocarcinoma. *C R Acad Sci III, 300*(8), 315-318.

Myzak, M. C., & Dashwood, R. H. (2006). Histone deacetylases as targets for dietary cancer preventive agents: lessons learned with butyrate, diallyl disulfide, and sulforaphane. *Curr Drug Targets, 7*(4), 443-452.

Nagarajan, R. P., & Costello, J. F. (2009). Epigenetic mechanisms in glioblastoma multiforme. *Semin Cancer Biol, 19*(3), 188-197.

Nowell, P. C. (1976). The clonal evolution of tumor cell populations. *Science, 194*(4260), 23-28.

Nowell, P. C., Rowley, J. D., & Knudson, A. G., Jr. (1998). Cancer genetics, cytogenetics--defining the enemy within. *Nat Med, 4*(10), 1107-1111.

Packer, E. I., & Hewang, R. J. (2012). Pediatric Brain Tumors (An Overview). *Pediatric Cancer*.pp1013-1022

Patel, M. R., & Tse, V. (2004). Diagnosis and staging of brain tumors. *Semin Roentgenol, 39*(3), 347-360.

Paulino, A. C. (2011). Pediatric Brain Tumors. *Decision making in Radiation oncology*, pp 1011-1035.

Kaganovich, D., Kopito, R., & Frydman, J. (2008). Misfolded proteins partition between two distinct quality control compartments. *Nature, 454*, 1088–1095.

Klionsky, D.J., Abdelmohsen, K., Abe, A., Abedin, M.J.,et al.(2016). Guidelines for the use and interpretation of assays for monitoring autophagy. *Autophagy, 12*(1),1-222.

Koukourakis, M.I., Kalamida, D., Giatromanolaki, A., Zois, C.E., et al.(2015). Autophagosome Proteins LC3A, LC3B and LC3C Have Distinct Subcellular Distribution Kinetics and Expression in Cancer Cell Lines. *PLoS One, 10*(9), 137675.

Richter-Landsberg, C., & Leyk, J. (2013). Inclusion body formation, macroautophagy, and the role of HDAC6 in neurodegeneration. *Acta Neuropathol, 126*(6), 793-807.

Rickert, C. H., & Paulus, W. (2001). Tumors of the choroid plexus. *Microsc Res Tech, 52*(1), 104-111.

Rodriguez-Gonzalez, A., Lin, T., Ikead, A. K., Simms-Waldrip, Fu,C
M.,(2008). Role of the Aggresome Pathway in Cancer: Targeting Histo
Dependent Protein Degradation. *Cancer Res, 68* (8), 2557-2560.

Roman, E. A., & Gonzalez Flecha, F. L. (2014). Kinetics and thermodynamics of membrane protein folding. *Biomolecules, 4*(1), 354-373.

Rosenfeldt, M. T., & Ryan, K. M. (2011). The multiple roles of autophagy in cancer. *Carcinogenesis, 32*(7), 955-963.

Saliba, R.S., Munro, P.M., Luthert, P.J., & Cheetham, M.E. (2002). The cellular fate of mutant rhodopsin: quality control, degradation and aggresome formation. *J Cell Sci., 115*, 2907–2918.

Sarkar, S., Carroll, B., Buganim, Y., Maetzel, D., Ng, A. H., Cassady, J. P., et al. (2013). Impaired autophagy in the lipid-storage disorder Niemann-Pick type C1 disease. *Cell Rep, 5*(5), 1302-1315.

Schmukler, E., Kloog, Y., & Pinkas-Kramarski, R. (2014). Ras and autophagy in cancer development and therapy. *Oncotarget, 5*(3), 577-586.

Sharma, S., Kelly, T. K., & Jones, P. A. (2010). Epigenetics in cancer. *Carcinogenesis, 31*(1), 27-36.

Shpilka, T., Weidberg, H., Pietrokovski, S., & Elazar, Z. (2011). Atg8: an autophagy-related ubiquitin-like protein family. *Genome Biol, 12* (7), 226.

Simoes-Pires, C., Zwick, V., Nurisso, A., Schenker, E., Carrupt, P. A., & Cuendet, M. (2013). HDAC6 as a target for neurodegenerative diseases: what makes it different from the other HDACs? *Mol Neurodegener, 8*, 7.

Spillantini, M. G., Schmidt, M. L., Lee, V. M., Trojanowski, J. Q., Jakes, R., & Goedert, M. (1997). Alpha-synuclein in Lewy bodies. *Nature, 388*(6645), 839-840.

Strazielle, N., & Ghersi-Egea, J. F. (2000). Choroid plexus in the central nervous system: biology and physiopathology. *J Neuropathol Exp Neurol, 59*(7), 561-574.

Strimpakos, A. S., Karapanagiotou, E. M., Saif, M. W., & Syrigos, K. N. (2009). The role of mTOR in the management of solid tumors: an overview. *Cancer Treat Rev, 35*(2), 148-159.

Surget, S.,Koury, M. P., Bourdon, J.C. (2013). Uncovering the role of p53 splice variants in human malignancy: a clinical perspective. *Onco Target Ther, 7*, 57-68.

Tabin, C. J., & Weinberg, R. A. (1985). Analysis of viral and somatic activations of the cHa-ras gene. *J Virol, 53*(1), 260-265.

Takalo, M., Salminen, A., Soininen, H., Hiltunen, M., & Haapasalo, A. (2013). Protein aggregation and degradation mechanisms in neurodegenerative diseases. *Am J Neurodegener Dis, 2*(1), 1-14.

Tan, J. M., Wong, E. S., Kirkpatrick, D. S., Pletnikova, O., Ko, H. S., Tay, S. P., et al. (2008). Lysine 63-linked ubiquitination promotes the formation and autophagic clearance of protein inclusions associated with neurodegenerative diseases. *Hum Mol Genet, 17*(3), 431-439.

Tanida, I., Ueno, T., & Kominami, E. (2004). LC3 conjugation system in mammalian autophagy. *Int J Biochem Cell Biol, 36*(12), 2503-2518.

Tanida, I., Minematsu-Ikeguchi, N., Ueno, T., Kominami, E. (2005).Lysosomal Turnover, but Not a Cellular Level, of Endogenous LC3 is a Marker for Autophagy. *Autophagy, 1*, 84–91.

Todde, V., Veenhuis, M., & van der Klei, I. J. (2009). Autophagy: principles and significance in health and disease. *Biochim Biophys Acta, 1792*(1), 3-13.

Verhoef, L., G. (2002). Aggregate formation inhibits proteasomal degradation of polyglutamine proteins. *Hum Mol Genet, 11*, 2689–2700.

Virani, S., Colacino, J. A., Kim, J. H., & Rozek, L. S. (2013). Cancer epigenetics: a brief review. *ILAR J, 53*(3-4), 359-369.

Wolburg, H., & Paulus, W. (2010). Choroid plexus: biology and pathology. *Acta Neuropathol, 119*(1), 75-88.

Yang, P. H., Zhang, L., Zhang, Y. J., Zhang, J., & Xu, W. F. (2013). HDAC6: physiological function and its selective inhibitors for cancer treatment. *Drug Discov Ther, 7*(6), 233-242.

Yao, T. P. (2010). The role of ubiquitin in autophagy-dependent protein aggregate processing. *Genes Cancer, 1*(7), 779-786.

Yap, T. A., Garrett, M. D., Walton, M. I., Raynaud, F., de Bono, J. S., & Workman, P. (2008). Targeting the PI3K-AKT-mTOR pathway: progress, pitfalls, and promises. *Curr Opin Pharmacol, 8*(4), 393-412.

Yu, X., Narayanan, S., Vazquez, A., & Carpizo, D. R. (2014). Small molecule compounds targeting the p53 pathway: are we finally making progress? *Apoptosis, 19*(7), 1055-1068.

Zaarur, N., Meriin, A.B., Bejarano, E., Xu, X., Gabai, V.L., et al. (2014). Proteasome Failure Promotes Positioning of Lysosomes around the Aggresome via Local Block of Microtubule-Dependent Transport. *Mol Cell Biol, 34, 1336*–1348.

Zaytseva, Y. Y., Valentino, J. D., Gulhati, P., & Evers, B. M. (2012). mTOR inhibitors in cancer therapy. *Cancer Lett, 319*(1), 1-7.

7-APPENDIX/COPYRIGHT FORMS

NATURE PUBLISHING GROUP LICENSE TERMS AND CONDITIONS

Mar 28, 2017

This Agreement between Marwa Nassar ("You") and Nature Publishing Group ("Nature Publishing Group") consists of your license details and the terms and conditions provided by Nature Publishing Group and Copyright Clearance Center.

License Number	4077581465380
License date	
Licensed Content Publisher	Nature Publishing Group
Licensed Content Publication	Oncogene
Licensed Content Title	A transcriptional variant of the LC3A gene is involved in autophagy and frequently inactivated in human cancers
Licensed Content Author	H Bai, J Inoue, T Kawano and J Inazawa
Licensed Content Date	Jan 16, 2012
Licensed Content Volume	31
Licensed Content Issue	40
Type of Use	reuse in a dissertation / thesis
Requestor type	non-commercial (non-profit)
Format	print and electronic
Portion	figures/tables/illustrations
Number of figures/tables/illustrations	1
High-res required	No
Figures	Figure 1 - a LC3 exon- intron structure
Author of this NPG article	No
Your reference number	
Title of your thesis / dissertation	Characterization of aggresomes formation in choroid plexus carcinoma
Expected completion date	Apr 2017
Estimated size (number of pages)	100
Requestor Location	Marwa Nassar 3A Saad Zalam street,Maadi Cairo, 342 Egypt Attn: Marwa Nassar
Billing Type	Invoice
Billing Address	Marwa Nassar 3A Saad Zalam street,Maadi Cairo, Egypt 342 Attn: Marwa Nassar
Total	0.00 USD
Terms and Conditions	

Terms and Conditions for Permissions

Nature Publishing Group hereby grants you a non-exclusive license to reproduce this material for this purpose, and for no other use,subject to the conditions below:

1. NPG warrants that it has, to the best of its knowledge, the rights to license reuse of this material. However, you should ensure that the material you are requesting is original to Nature Publishing Group and does not carry the copyright of another entity (as credited in the published version). If the credit line on any part of the material you have requested indicates that it was reprinted or adapted by NPG with permission from another source, then you should also seek permission from that source to reuse the material.

2. Permission granted free of charge for material in print is also usually granted for any electronic version of that work, provided that the material is incidental to the work as a whole and that the electronic version is essentially equivalent to, or substitutes for, the print version.Where print permission has been granted for a fee, separate permission must be obtained for any additional, electronic re-use (unless, as in the case of a full paper, this has already been accounted for during your initial request in the calculation of a print run).NB: In all cases, web-based use of full-text articles must be authorized separately through the 'Use on a Web Site' option when requesting permission.

3. Permission granted for a first edition does not apply to second and subsequent editions and for editions in other languages (except for signatories to the STM Permissions Guidelines, or where the first edition permission was granted for free).

4. Nature Publishing Group's permission must be acknowledged next to the figure, table or abstract in print. In electronic form, this acknowledgement must be visible at the same time as the figure/table/abstract, and must be hyperlinked to the journal's homepage.

5. The credit line should read:
   Reprinted by permission from Macmillan Publishers Ltd: [JOURNAL NAME] (reference citation), copyright (year of publication)
   For AOP papers, the credit line should read:
   Reprinted by permission from Macmillan Publishers Ltd: [JOURNAL NAME], advance online publication, day month year (doi: 10.1038/sj.[JOURNAL ACRONYM].XXXXX)

   Note: For republication from the *British Journal of Cancer,* the following credit lines apply.
   Reprinted by permission from Macmillan Publishers Ltd on behalf of Cancer Research UK: [JOURNAL NAME] (reference citation), copyright (year of publication)For AOP papers, the credit line should read:
   Reprinted by permission from Macmillan Publishers Ltd on behalf of Cancer Research UK: [JOURNAL NAME], advance online publication, day month year (doi: 10.1038/sj.[JOURNAL ACRONYM].XXXXX)

6. Adaptations of single figures do not require NPG approval. However, the adaptation should be credited as follows:

   Adapted by permission from Macmillan Publishers Ltd: [JOURNAL NAME] (reference citation), copyright (year of publication)

   Note: For adaptation from the *British Journal of Cancer,* the following credit line applies.
   Adapted by permission from Macmillan Publishers Ltd on behalf of Cancer Research UK: [JOURNAL NAME] (reference citation), copyright (year of publication)

7. Translations of 401 words up to a whole article require NPG approval. Please visit http://www.macmillanmedicalcommunications.com for more information.Translations of up to a 400 words do not require NPG approval. The translation should be credited as follows:

   Translated by permission from Macmillan Publishers Ltd: [JOURNAL NAME] (reference citation), copyright (year of publication).

   Note: For translation from the *British Journal of Cancer,* the following

credit line applies.
Translated by permission from Macmillan Publishers Ltd on behalf of Cancer Research UK: [JOURNAL NAME] (reference citation), copyright (year of publication)

We are certain that all parties will benefit from this agreement and wish you the best in the use of this material. Thank you.
Special Terms:
v1.1

AMERICAN ASSOCIATION FOR CANCER RESEARCH LICENSE TERMS AND CONDITIONS

Mar 28, 2017

This Agreement between Marwa Nassar ("You") and American Association for Cancer Research ("American Association for Cancer Research") consists of your license details and the terms and conditions provided by American Association for Cancer Research and Copyright Clearance Center.

License Number	4077580315342
License date	
Licensed Content Publisher	American Association for Cancer Research
Licensed Content Publication	Cancer Research
Licensed Content Title	Role of the Aggresome Pathway in Cancer: Targeting Histone Deacetylase 6–Dependent Protein Degradation
Licensed Content Author	Agustin Rodriguez-Gonzalez,Tara Lin,Alan K. Ikeda,Tiffany Simms-Waldrip,Cecilia Fu,Kathleen M. Sakamoto
Licensed Content Date	2008-04-15
Licensed Content Volume	68
Licensed Content Issue	8
Type of Use	Thesis/Dissertation
Requestor type	non-commercial (non-profit)
Format	print and electronic
Portion	figures/tables/illustrations
Number of figures/tables/illustrations	1
Will you be translating?	No
Circulation	500
Territory of distribution	Worldwide
Title of your thesis / dissertation	Characterization of aggresomes formation in choroid plexus carcinoma
Expected completion date	Apr 2017
Estimated size (number of pages)	100
Requestor Location	Marwa Nassar 3A Saad Zalam street,Maadi Cairo, 342 Egypt Attn: Marwa Nassar
Billing Type	Invoice
Billing Address	Marwa Nassar 3A Saad Zalam street,Maadi Cairo, Egypt 342 Attn: Marwa Nassar

Total 0.00 USD

Terms and Conditions

American Association for Cancer Research (AACR) Terms and Conditions

INTRODUCTION

The Publisher for this copyright material is the American Association for Cancer Research (AACR). By clicking "accept" in connection with completing this licensing transaction, you agree to the following terms and conditions applying to this transaction. You also agree to the Billing and Payment terms and conditions established by Copyright Clearance Center (CCC) at the time you opened your Rightslink account.

LIMITED LICENSE

The AACR grants exclusively to you, the User, for onetime, non-exclusive use of this material for the purpose stated in your request and used only with a maximum distribution equal to the number you identified in the permission process. Any form of republication must be completed within one year although copies made before then may be distributed thereafter and any electronic posting is limited to a period of one year. Reproduction of this material is confined to the purpose and/or media for which permission is granted. Altering or modifying this material is not permitted. However, figures and illustrations may be minimally altered or modified to serve the new work.

GEOGRAPHIC SCOPE

Licenses may be exercised as noted in the permission process

RESERVATION OF RIGHTS

The AACR reserves all rights not specifically granted in the combination of 1) the license details provided by you and accepted in the course of this licensing transaction, 2) these terms and conditions , and 3) CCC's Billing and Payment terms and conditions.

DISCLAIMER

You may obtain permission via Rightslink to use material owned by AACR. When you are requesting permission to reuse a portion for an AACR publication, it is your responsibility to examine each portion of content as published to determine whether a credit to, or copyright notice of a third party owner is published next to the item. You must obtain permission from the third party to use any material which has been reprinted with permission from the said third party. If you have not obtained permission from the third party, AACR disclaims any responsibility for the use you make of items owned by them.

LICENSE CONTINGENT ON PAYMENT

While you may exercise the rights licensed immediately upon issuance of the license at the end of the licensing process for the transaction, provided that you have disclosed complete and accurate details of your proposed use, no license is finally effective unless and until full payment is received from you, either by the publisher or by the CCC, as provided in CCC's Billing and Payment terms and conditions. If full payment is not received on a timely basis, then any license preliminarily granted shall be deemed automatically revoked and shall be void as if never granted. Further, in the event that you breach any of these terms and

conditions, or any of the CCC's Billing and Payment terms and conditions, the license is automatically revoked and shall be void as if never granted. Use of materials as described in a revoked license, as well as any use of the materials beyond the scope of an unrevoked license, may constitute copyright infringement and the publisher reserves the right to take any and all action to protect its copyright in the materials.

COPYRIGHT NOTICE

You must include the following credit line in connection with your reproduction of the licensed material: "Reprinted (or adapted) from Publication Title, Copyright Year, Volume/Issue, Page Range, Author, Title of Article, with permission from AACR".

TRANSLATION

This permission is granted for non-exclusive world English rights only.

WARRANTIES

Publisher makes no representations or warranties with respect to the licensed material.

INDEMNIFICATION

You hereby indemnify and agree to hold harmless the publisher and CCC, and their respective officers, directors, employees and agents, from and against any and all claims arising out of your use of the licensed material other than as specifically authorized pursuant to this license.

REVOCATION

The AACR reserves the right to revoke a license for any reason, including but not limited to advertising and promotional uses of AACR content, third party usage and incorrect figure source attribution.

NO TRANSFER OF LICENSE

This license is personal to you and may not be sublicensed, assigned, or transferred by you to any other person without publisher's written permission.

NO AMENDMENT EXCEPT IN WRITING

This license may not be amended except in a writing signed by both parties (or, in the case of publisher, by CCC on publisher's behalf).

OBJECTION TO CONTRARY TERMS

Publishers hereby objects to any terms contained in any purchase order, acknowledgement, check endorsement or other writing prepared by you, which terms are inconsistent with these terms and conditions or CCC's Billing and Payment terms and conditions. These terms and conditions together with CCC's Billing and Payment terms and conditions (which are incorporated herein) comprise the entire agreement between you and publisher (and CCC) concerning this licensing transaction. In the event of any conflict between your obligations established by these terms and conditions, and those established by CCC's Billing and Payment terms and conditions, these terms and conditions shall control.

THESIS/DISSERTATION TERMS

If your request is to reuse an article authored by you and published by the AACR in your dissertation/thesis, your thesis may be submitted to your institution in either in print or electronic form. Should your thesis be published commercially, please reapply.

ELECTRONIC RESERVE

If this license is made in connection with a course, and the Licensed Material or any portion thereof is to be posted to a website, the website is to be password protected and made available only to the students registered for the relevant course. The permission is granted for the duration of the course. All content posted to the website must maintain the copyright information notice.

JURISDICTION

This license transaction shall be governed by and construed in accordance with the laws of Pennsylvania. You hereby agree to submit to the jurisdiction of the federal and state courts located in Pennsylvania for purposes of resolving any disputes that may arise in connection with this licensing transaction.

Other Terms and Conditions:

v1.0

BIOSCIENTIFICA LTD. LICENSE TERMS AND CONDITIONS

Mar 28, 2017

This Agreement between Marwa Nassar ("You") and BioScientifica Ltd. ("BioScientifica Ltd.") consists of your license details and the terms and conditions provided by BioScientifica Ltd. and Copyright Clearance Center.

License Number	4077200853006
License date	
Licensed Content Publisher	BioScientifica Ltd.
Licensed Content Publication	Journal of Molecular Endocrinology
Licensed Content Title	Linking the ubiquitin–proteasome pathway to chromatin remodeling/modification by nuclear receptors
Licensed Content Author	H K Kinyamu, J Chen, T K Archer et al.
Licensed Content Date	Apr 1, 2005
Licensed Content Volume	34
Licensed Content Issue	2
Type of Use	Thesis/Dissertation
Requestor type	Publisher, not-for-profit
Format	Print, Electronic
Portion	image/photo
Number of images/photos requested	1
Rights for	Main product
Duration of use	Life of current edition
Creation of copies for the disabled	no
With minor editing privileges	yes
For distribution to	Worldwide
In the following language(s)	Original language of publication
With incidental promotional use	no
The lifetime unit quantity of new product	0 to 499
The requesting person/organization is:	American university in Cairo
Order reference number	
Title of your thesis / dissertation	Characterization of aggresomes formation in choroid plexus carcinoma
Expected completion date	Apr 2017
Expected size (number of pages)	100
Requestor Location	Marwa Nassar 3A Saad Zalam street,Maadi Cairo, 342

	Egypt Attn: Marwa Nassar
Publisher Tax ID	GB 869 9945 28
Billing Type	Invoice
Billing Address	Marwa Nassar 3A Saad Zalam street,Maadi Cairo, Egypt 342 Attn: Marwa Nassar
Total	0.00 GBP

Terms and Conditions

Introduction

The publisher for this copyrighted material is Bioscientifica Ltd. By clicking "accept" in connection with completing this licensing transaction, you agree that the following terms and conditions apply to this transaction (along with the Billing and Payment terms and conditions established by Copyright Clearance Center, Inc. ("CCC"), at the time that you opened your CCC account and that are available at any time at).

Limited License

The publisher hereby grants to you a non-exclusive license to use this material. Licenses are for one-time use only with a maximum distribution equal to the number that you identified in the licensing process.

Geographic Rights: Scope

Licenses may be exercised anywhere in the world.

Reservation of Rights

The publisher reserves all rights not specifically granted in the combination of (i) the license details provided by you and accepted in the course of this licensing transaction, (ii) these terms and conditions and (iii) CCC's Billing and Payment terms and conditions.

Limited Contingent on Payment

While you may exercise the rights licensed immediately upon issuance of the license at the end of the licensing process for the transaction, provided that you have disclosed complete and accurate details of your proposed use, no license is finally effective unless and until full payment is received from you (either by publisher or by CCC) as provided in CCC's Billing and Payment terms and conditions. If full payment is not received on a timely basis, then any license preliminarily granted shall be deemed automatically revoked and shall be void as if never granted. Further, in the event that you breach any of these terms and conditions or any of CCC's Billing and Payment terms and conditions, the license is automatically revoked and shall be void as if never granted. Use of materials as described in a revoked license, as well as any use of the materials beyond the scope of an unrevoked license, may constitute copyright infringement and publisher reserves the right to take any and all action to protect its copyright in the materials.

Copyright NoticeYou must include the following copyright and permission notice in connection with any reproduction of the licensed

material: "Copyright [Original year of publication] [Copyright holder]."
Warranties: None
The publisher makes no representations or warranties with respect to the licensed material and adopts on its own behalf the limitations and disclaimers established by CCC on its behalf in its Billing and Payment terms and conditions for this licensing transaction.
Indemnity
You hereby indemnify and agree to hold harmless the publisher and CCC, and their respective officers, directors, employees and agents, from and against any and all claims arising out of your use of the licensed material other than as specifically authorized pursuant to this license. In no event shall the publisher or CCC be liable for any special, incidental, indirect or consequential damages of any kind arising out of or in connection with the use of the articles or other material derived from the journals, whether or not advised of the possibility of damage, and on any theory of liability.
No Transfer of License
This license is personal to you and may not be sublicensed, assigned, or transferred by you to any other person without the publisher's written permission.
No Amendment Except in Writing
This license may not be amended except in a writing signed by both parties (or, in the case of the publisher, by CCC on publisher's behalf).
Objection to Contrary Terms
The publisher hereby objects to any terms contained in any purchase order, acknowledgment, check endorsement or other writing prepared by you, which terms are inconsistent with these terms and conditions or CCC's Billing and Payment terms and conditions. These terms and conditions, together with CCC's Billing and Payment terms and conditions (which are incorporated herein), comprise the entire agreement between you and publisher (and CCC) concerning this licensing transaction. In the event of any conflict between your obligations established by these terms and conditions and those established by CCC's Billing and Payment terms and conditions, these terms and conditions shall control.
STM Permissions Guidelines
The publisher is a signatory to the STM Guidelines and as such grants permission to other signatory STM publishers to re-use material strictly in accordance with the current STM Guidelines (http://www.stm-assoc.org/permissions-guidelines/).
Other Terms and Conditions:
V.1 10.26/12

AMERICAN ASSOCIATION FOR CANCER RESEARCH LICENSE TERMS AND CONDITIONS

Mar 28, 2017

This Agreement between Marwa Nassar ("You") and American Association for Cancer Research ("American Association for Cancer Research") consists of your license details and the terms and conditions provided by American Association for Cancer Research and Copyright Clearance Center.

License Number	4077600049559
License date	
Licensed Content Publisher	American Association for Cancer Research
Licensed Content Publication	Molecular Cancer Therapeutics
Licensed Content Title	Picking the Point of Inhibition: A Comparative Review of PI3K/AKT/mTOR Pathway Inhibitors
Licensed Content Author	Rodrigo Dienstmann,Jordi Rodon,Violeta Serra,Josep Tabernero
Licensed Content Date	2014-05-01
Licensed Content Volume	13
Licensed Content Issue	5
Type of Use	Thesis/Dissertation
Requestor type	non-commercial (non-profit)
Format	print and electronic
Portion	figures/tables/illustrations
Number of figures/tables/illustrations	1
Will you be translating?	No
Circulation	500
Territory of distribution	Worldwide
Title of your thesis / dissertation	Characterization of aggresomes formation in choroid plexus carcinoma
Expected completion date	Apr 2017
Estimated size (number of pages)	100
Requestor Location	Marwa Nassar 3A Saad Zalam street,Maadi Cairo, 342 Egypt Attn: Marwa Nassar
Billing Type	Invoice
Billing Address	Marwa Nassar 3A Saad Zalam street,Maadi Cairo, Egypt 342 Attn: Marwa Nassar
Total	0.00 USD

American Association for Cancer Research (AACR) Terms and Conditions

INTRODUCTION

The Publisher for this copyright material is the American Association for Cancer Research (AACR). By clicking "accept" in connection with completing this licensing transaction, you agree to the following terms and conditions applying to this transaction. You also agree to the Billing and Payment terms and conditions established by Copyright Clearance Center (CCC) at the time you opened your Rightslink account.

LIMITED LICENSE

The AACR grants exclusively to you, the User, for onetime, non-exclusive use of this material for the purpose stated in your request and used only with a maximum distribution equal to the number you identified in the permission process. Any form of republication must be completed within one year although copies made before then may be distributed thereafter and any electronic posting is limited to a period of one year. Reproduction of this material is confined to the purpose and/or media for which permission is granted. Altering or modifying this material is not permitted. However, figures and illustrations may be minimally altered or modified to serve the new work.

GEOGRAPHIC SCOPE

Licenses may be exercised as noted in the permission process

RESERVATION OF RIGHTS

The AACR reserves all rights not specifically granted in the combination of 1) the license details provided by you and accepted in the course of this licensing transaction, 2) these terms and conditions , and 3) CCC's Billing and Payment terms and conditions.

DISCLAIMER

You may obtain permission via Rightslink to use material owned by AACR. When you are requesting permission to reuse a portion for an AACR publication, it is your responsibility to examine each portion of content as published to determine whether a credit to, or copyright notice of a third party owner is published next to the item. You must obtain permission from the third party to use any material which has been reprinted with permission from the said third party. If you have not obtained permission from the third party, AACR disclaims any responsibility for the use you make of items owned by them.

LICENSE CONTINGENT ON PAYMENT

While you may exercise the rights licensed immediately upon issuance of the license at the end of the licensing process for the transaction, provided that you have disclosed complete and accurate details of your proposed use, no license is finally effective unless and until full payment is received from you, either by the publisher or by the CCC, as provided in CCC's Billing and Payment terms and conditions. If full payment is not received on a timely basis, then any license preliminarily granted shall be deemed automatically revoked and shall be void as if never granted. Further, in the event that you breach any of these terms and conditions, or any of the CCC's Billing and Payment terms and conditions, the license is automatically revoked and shall be void as if

never granted. Use of materials as described in a revoked license, as well as any use of the materials beyond the scope of an unrevoked license, may constitute copyright infringement and the publisher reserves the right to take any and all action to protect its copyright in the materials.

COPYRIGHT NOTICE

You must include the following credit line in connection with your reproduction of the licensed material: "Reprinted (or adapted) from Publication Title, Copyright Year, Volume/Issue, Page Range, Author, Title of Article, with permission from AACR".

TRANSLATION

This permission is granted for non-exclusive world English rights only.

WARRANTIES

Publisher makes no representations or warranties with respect to the licensed material.

INDEMNIFICATION

You hereby indemnify and agree to hold harmless the publisher and CCC, and their respective officers, directors, employees and agents, from and against any and all claims arising out of your use of the licensed material other than as specifically authorized pursuant to this license.

REVOCATION

The AACR reserves the right to revoke a license for any reason, including but not limited to advertising and promotional uses of AACR content, third party usage and incorrect figure source attribution.

NO TRANSFER OF LICENSE

This license is personal to you and may not be sublicensed, assigned, or transferred by you to any other person without publisher's written permission.

NO AMENDMENT EXCEPT IN WRITING

This license may not be amended except in a writing signed by both parties (or, in the case of publisher, by CCC on publisher's behalf).

OBJECTION TO CONTRARY TERMS

Publishers hereby objects to any terms contained in any purchase order, acknowledgement, check endorsement or other writing prepared by you, which terms are inconsistent with these terms and conditions or CCC's Billing and Payment terms and conditions. These terms and conditions together with CCC's Billing and Payment terms and conditions (which are incorporated herein) comprise the entire agreement between you and publisher (and CCC) concerning this licensing transaction. In the event of any conflict between your obligations established by these terms and conditions, and those established by CCC's Billing and Payment terms and conditions, these terms and conditions shall control.

THESIS/DISSERTATION TERMS

If your request is to reuse an article authored by you and published by the AACR in your dissertation/thesis, your thesis may be submitted to your institution in either in print or electronic form. Should your thesis be published commercially, please reapply.

ELECTRONIC RESERVE

If this license is made in connection with a course, and the Licensed Material or any portion thereof is to be posted to a website, the website

is to be password protected and made available only to the students registered for the relevant course. The permission is granted for the duration of the course. All content posted to the website must maintain the copyright information notice.

JURISDICTION

This license transaction shall be governed by and construed in accordance with the laws of Pennsylvania. You hereby agree to submit to the jurisdiction of the federal and state courts located in Pennsylvania for purposes of resolving any disputes that may arise in connection with this licensing transaction.

Other Terms and Conditions:

v1.0

Open Access:

Confirmation Number: 11634397
Order Date: 03/27/2017

Customer Information

Customer: Marwa Nassar
Account Number: 3001130851
Organization: Marwa Nassar
Email: marwanassar4@aucegypt.edu
Phone: +20 105230395

Order Details

OncoTargets and Therapy

Billing Status:
N/A

- **Order detail ID:**70370741
- **ISSN:**1178-6930
- **Publication Type:**e-Journal
- **Volume:**
- **Issue:**
- **Start page:**
- **Publisher:**Dove Medical Press
- **Permission Status:** **Granted**
- **Permission type:**Republish or display content
- **Type of use:**Republish in a thesis/dissertation

Order License Id: 4077200613859

- Hide details

Requestor type	Publisher, not-for-profit
Format	Print, Electronic
Portion	image/photo
Number of images/photos requested	1
Title or numeric reference of the portion(s)	Figure 1, P53 pathway
Title of the article or chapter the portion is from	Uncovering the role of p53 splice variants in human malignancy: a clinical perspective
Editor of portion(s)	n/a
Author of portion(s)	surget S
Volume of serial or monograph	n/a
Page range of portion	2013
Publication date of portion	2013
Rights for	Main product
Duration of use	Life of current edition
Creation of copies for the disabled	no
With minor editing privileges	yes
For distribution to	Worldwide
In the following language(s)	Original language of publication
With incidental promotional use	no
Lifetime unit quantity of new product	Up to 499
Made available in the following markets	education
The requesting person/organization	Marwa Nassar
Order reference number	
Author/Editor	Marwa Nassar
The standard identifier of New Work	Marwa2
Title of New Work	Charachterisation of aggresome formation in choroid plexus carcinoma
Publisher of New Work	American university in cairo
Expected publication date	Apr 2017

Estimated size (pages) 100

Note: This item was invoiced separately through our **RightsLink service.** More info **$ 0.00**

Total order items: 1

Order Total: $0.00